

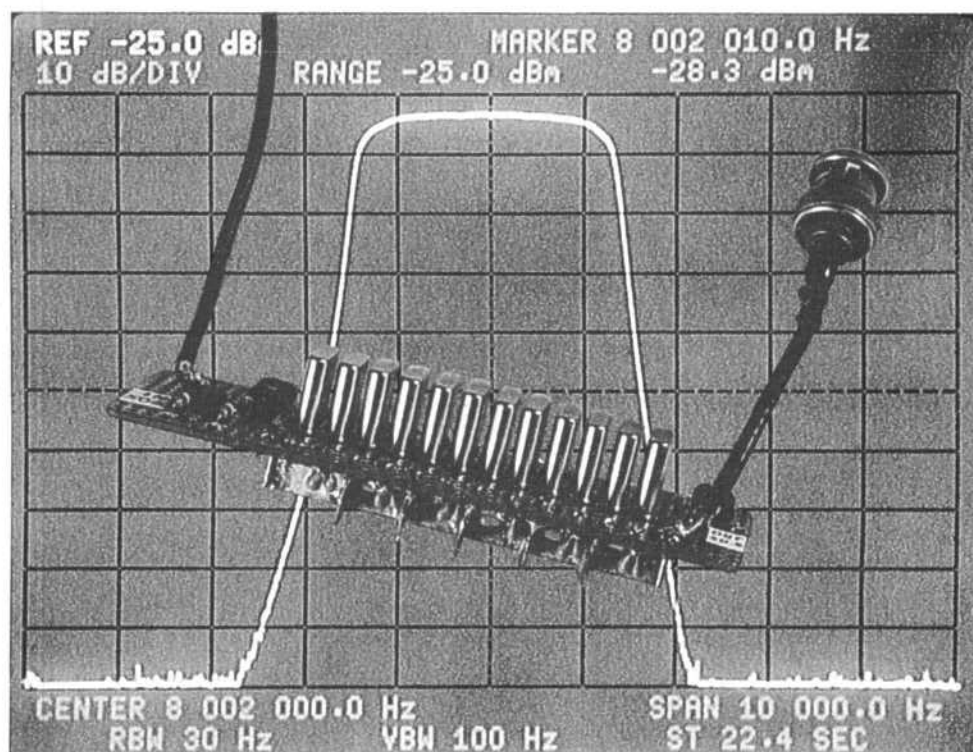
QEX

\$1.75



ARRL Experimenter's Exchange

January 1995



Crystal Filters via Computer

QEX: The ARRL
Experimenter's Exchange
American Radio Relay League
225 Main Street
Newington, CT USA 06111

QEX

QEX (ISSN: 0886-8093 USPS 011-424) is published monthly by the American Radio Relay League, Newington, CT USA.

Second-class postage paid at Hartford, Connecticut and additional mailing offices.

David Sumner, K1ZZ
Publisher

Jon Bloom, KE3Z
Editor

Lori Weinberg
Assistant Editor

Harold Price, NK6K
Zack Lau, KH6CP
Contributing Editors

Production Department

Mark J. Wilson, AA2Z
Publications Manager

Michelle Bloom, WB1ENT
Production Supervisor

Sue Fagan
Graphic Design Supervisor

Joe Costa
Technical Illustrator

Joe Shea
Production Assistant

Advertising Information Contact:

Brad Thomas, KC1EX, Advertising Manager
American Radio Relay League
203-667-2494 direct
203-666-1541 ARRL
203-665-7531 fax

Circulation Department

Debra Jahnke, Manager
Kathy Fay, N1GZO, Deputy Manager
Cathy Stepina, QEX Circulation

Offices

225 Main St, Newington, CT 06111-1494 USA
Telephone: 203-666-1541
Telex: 650215-5052 MCI
FAX: 203-665-7531 (24 hour direct line)
Electronic Mail: MCIMAILID: 215-5052
Internet: qex@arrl.org

Subscription rate for 12 issues:

In the US: ARRL Member \$12,
nonmember \$24;

US, Canada and Mexico by First Class Mail:
ARRL Member \$25, nonmember \$37;

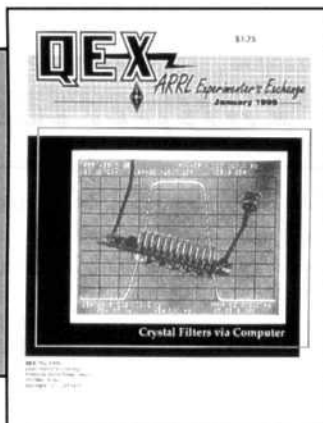
Elsewhere by Surface Mail (4-8 week
delivery): ARRL Member \$20,
nonmember \$32;

Elsewhere by Airmail: ARRL Member \$48,
nonmember \$60.

QEX subscription orders, changes of address, and reports of missing or damaged copies may be marked: QEX Circulation. Postmaster: Form 3579 requested. Send change of address to: American Radio Relay League, 225 Main St, Newington, CT 06111-1494.

Members are asked to include their membership control number or a label from their QST wrapper when applying.

Copyright © 1994 by the American Radio Relay League Inc. Material may be excerpted from QEX without prior permission provided that the original contributor is credited, and QEX is identified as the source.



About the Cover

Computer-aided design makes home construction of even tricky circuits like crystal filters possible, as N6NWP shows us this month.

ISSUE
NO.
155



Features

3 Designing and Building High-Performance Crystal Ladder Filters

By Jacob Makhinson, N6NWP

18 High-Performance Antennas for 5760 MHz

By Paul Wade, N1BWT

22 Effects of the Ionosphere

By Jacques d'Avignon, VE3VIA

Columns

26 RF

By Zack Lau, KH6CP/1

January 1995 QEX Advertising Index

American Radio Relay League: 31, 32,
Cov IV
Communications Specialists Inc: 30
LUCAS Radio/Kangaroo Tabor
Software: 30

PacComm: Cov II, Cov III
PC Electronics: 17
Tucson Amateur Packet Radio Corp: 30
Z Domain Technologies, Inc: 30



The American Radio Relay League, Inc. is a noncommercial association of radio amateurs, organized for the promotion of interests in Amateur Radio communication and experimentation, for the establishment of networks to provide communications in the event of disasters or other emergencies, for the advancement of radio art and of the public welfare, for the representation of the radio amateur in legislative matters, and for the maintenance of fraternalism and a high standard of conduct.

ARRL is an incorporated association without capital stock chartered under the laws of the state of Connecticut, and is an exempt organization under Section 501(c)(3) of the Internal Revenue Code of 1986. Its affairs are governed by a Board of Directors, whose voting members are elected every two years by the general membership. The officers are elected or appointed by the Directors. The League is noncommercial, and no one who could gain financially from the shaping of its affairs is eligible for membership on its Board.

"Of, by, and for the radio amateur," ARRL numbers within its ranks the vast majority of active amateurs in the nation and has a proud history of achievement as the standard-bearer in amateur affairs.

A bona fide interest in Amateur Radio is the only essential qualification of membership; an Amateur Radio license is not a prerequisite, although full voting membership is granted only to licensed amateurs in the US.

Membership inquiries and general correspondence should be addressed to the administrative headquarters at 225 Main Street, Newington, CT 06111 USA.

Telephone: 203-666-1541
Telex: 650215-5052 MCI
MCIMAIL (electronic mail system) ID: 215-5052
FAX: 203-665-7531 (24-hour direct line)

Officers

President: GEORGE S. WILSON III, W4OYI
1649 Griffith Ave, Owensboro, KY 42301

Executive Vice President: DAVID SUMNER, K1ZZ

Purpose of QEX:

- 1) provide a medium for the exchange of ideas and information between Amateur Radio experimenters
- 2) document advanced technical work in the Amateur Radio field
- 3) support efforts to advance the state of the Amateur Radio art

All correspondence concerning QEX should be addressed to the American Radio Relay League, 225 Main Street, Newington, CT 06111 USA. Envelopes containing manuscripts and correspondence for publication in QEX should be marked: Editor, QEX.

Both theoretical and practical technical articles are welcomed. Manuscripts should be typed and doubled spaced. Please use the standard ARRL abbreviations found in recent editions of *The ARRL Handbook*. Photos should be glossy, black and white positive prints of good definition and contrast, and should be the same size or larger than the size that is to appear in QEX.

Any opinions expressed in QEX are those of the authors, not necessarily those of the editor or the League. While we attempt to ensure that all articles are technically valid, authors are expected to defend their own material. Products mentioned in the text are included for your information; no endorsement is implied. The information is believed to be correct, but readers are cautioned to verify availability of the product before sending money to the vendor.

Empirically Speaking

AMSAT's Phase IIID Satellite

One of the most amazing aspects of Amateur Radio over the past three decades has been the ability of amateurs to get their own satellites into orbit. The fact that we've been able to solve the technical problems of building and operating satellites is not nearly as surprising as our ability to get the "birds" paid for and launched. This is in no way to minimize the contributions of the small core of dedicated amateurs who do the technical work—without them there would be no amateur satellites. But the cost of building satellites to launch-agency specifications and the scarcity and cost of the launches themselves have always been the least tractable problems. Yet, somehow, amateurs keep getting their satellites built and sent aloft.

As amateurs keep building satellites, the capability of those satellites increases. Now, several AMSAT organizations are banding together to build the most capable amateur satellite yet: Phase IIID (P3D). While previous satellites had one or a few hard-wired transponders, P3D is slated to have a *matrix* of transponders, allowing unprecedented flexibility in selection of uplink and downlink bands. Uplinks will be on 2 m, 70 cm, 23 cm, 13 cm and 5 cm, and the downlink bands are 2 m, 70 cm, 13 cm, 3 cm and 1.25 cm. The switching matrix will allow transponder configuration of any uplink band with virtually any downlink band (except the same band).

Along with the unprecedented band selection capability, P3D will have 3-axis stabilization, allowing use of high-gain antennas, and powerful transmitters. This will permit operation through its transponders using reasonable ground transmitter power levels and ground receiving systems and antennas. Accessing P3D should be easier than with any previous satellite.

Another exciting innovation P3D will bring is its RUDAK-U digital transponder. Comprising two independent computers, each with 16 megabytes of memory and PC-type processing power, RUDAK-U will provide multiple digital uplinks and downlinks that include existing digital satellite protocols (1200 and 9600 baud), as well as DSP-based

modems that can adapt to new technology on the ground.

Aside from P3D being a powerful communication tool, and a fun high-tech amateur mode, its presence—and that of its users—on the amateur microwave bands can play a part in saving those frequencies from further encroachment by other services. So, even if satellites are not your "thing" you may have a vested interest in seeing P3D glittering in the sky.

But, as we said, the most problematic part of making a capable amateur satellite is not the design and construction; it's the money. And that's where you come in. (You knew this was coming.) Without a solid base of financial support from the amateur community, no amateur satellite—including P3D—can get launched. If you hope to see amateur technology pushed forward by the presence of a more capable satellite in orbit, now is the time to help make that happen. With the 1996 launch date rapidly approaching, "crunch time" for the fund-raising effort is *now*. To contribute to P3D, send your contributions (and questions) to: AMSAT, 850 Sligo Ave, Silver Spring, MD 20910.

This Month in QEX

"Designing and Building High-Performance Crystal Ladder Filters" may seem like black magic to many, but Jacob Makhinson, N6NWP, provides a look behind the magician's curtain with the aid of computer design tools.

We've presented a number of circuits for 5760 MHz over the last year or so. Now how about some antennas to go with them? Paul Wade, N1BWT obliges with "High-Performance Antennas for 5760 MHz."

HF propagation plays havoc with many kinds of signals, but perhaps no mode shows the "Effects of the Ionosphere" quite as well as does facsimile. Jacques d'Avignon, VE3VIA, has thoroughly analyzed one facsimile reception incident, showing in detail why "strong signals" and "good signals" are not always the same thing.

A low-noise preamp isn't ensured by using a low-noise device. You also need a good input network, such as that used in the half-wave cavity designs presented by Zack Lau, KH6CP/1 in this month's "RF column.—KE3Z, email: jbloom@arrl.org (Internet)

Designing and Building High-Performance Crystal Ladder Filters

*Designing crystal filters for SSB is made
easier using readily available software.*

By Jacob Makhinson, N6NWP

Despite the several excellent articles about crystal filters that have been published in amateur magazines over the years, building high-quality crystal filters is still seen by many amateurs as either black magic or as a complicated procedure beyond the reach of the average builder.

A crystal filter, being the heart of a superheterodyne receiver, has a profound effect on its selectivity. A low-quality crystal filter in even a high-priced commercial transceiver can degrade its selectivity and dynamic range. On the other hand, a good crystal filter can significantly enhance receiver performance, whether in a simple "weekend" project or in a competition-grade station.

Commercially available crystal filters are usually expensive and often discourage construction-minded amateurs from pursuing projects that include crystal filters. In addition, studies conducted in recent years conclude that in a high-performance receiver, a crystal filter may become the "bottleneck" restricting the receiver's dynamic range. So, the goal of this article is to provide design and building methods that can be used to construct crystal filters that rival or exceed the quality of commercially available filters. I will describe a simple, practical step-by-step procedure to design, construct and align crystal filters using equipment available to most construction-minded amateurs. The resulting filters achieve top-quality performance at a fraction of the cost of commercially available crystal filters.

Most of the crystal filters described

in amateur projects and those being sold commercially are lattice, half-lattice or cascaded half-lattice filters like those shown in Fig 1. A two- or four-crystal filter of this type can provide a symmetrical response with reasonably steep skirts. But the bandwidth of such filters is a function of the frequency separation of the crystals. If a steeper response is desired, designing a half-lattice filter with more than four crystals becomes more complex, requiring matched pairs of crystals and several adjustments. While it is reasonably easy to obtain matched crystal pairs for CW filters, it becomes considerably more problematic to obtain pairs of crystals separated by a couple of thousand hertz for use in SSB filters. In addition, the coils used for lattice filter alignment often use small cores, which can result in the degradation of dynamic range because of core saturation at high signal levels.

Another form of filter—which is the subject of this article—is the ladder filter shown in Fig 2. It typically has an asymmetrical response and is sometimes called the “lower-sideband ladder” configuration. But as we’ll see, with a sufficient number of poles this asymmetry is significantly reduced. Ladder filters offer several advantages to the amateur experimenter:

- there is no need to pick crystals for proper frequency separation and no need for matched crystal pairs;
- the inherently simpler filter topology results in simple construction methods;
- no adjustable components are required after alignment is completed;
- the absence of coils allows a compact assembly and reduces the possibility of dynamic range degradation;
- the simple topology is conducive to a high number of poles, which allows very steep skirts; and

- a computer program is available that eliminates the need for empirical approaches or cut-and-try methods and allows the designer to shape the filter response with great accuracy.

This work was inspired by an article by Bill Carver, K6OLG/7.¹ Carver’s work is quite remarkable; first, it proves that it is possible to build high-quality CW and SSB crystal filters with a predetermined frequency response “without black magic,” and second (but of no less importance), it proves that the performance of filters built in a home lab using home-built equipment successfully rivals that of filters built using sophisticated professional equipment.

This article builds on Carver’s work, refines the crystal filter design criteria and methodology, walks the reader through a complete design example, provides the results of measurements on several crystal ladder filters and analyzes the results.

The scope of this study has been limited to SSB filters, although most of the methods and conclusions are also applicable to CW filters.

The computer-design stage is based on a collection of computer programs designed by Wes Hayward, W7ZOI. The ARRL has just republished Wes Hayward’s textbook *Introduction to Radio Frequency Design*, now including the software as part of the package.² The computer programs (which I will refer to as *IRFD*) run on an IBM PC or compatible computer. The computer requirements are minimal, since *IRFD* fits on a single floppy disk and the computer’s speed is of no concern. A VGA card is required for graphic display, however.

The Design Procedure

Design and construction of these ladder crystal filters are performed using these steps:

- selection of the filter center frequency;
- measurement of crystal parameters;

¹Notes appear on page 17.

- selection of the shape of the response;
- computer design of the filter; and
- construction and alignment.

Frequency Selection

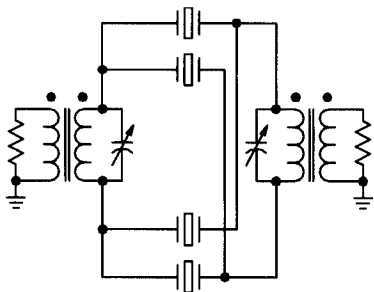
If the required filter frequency is not already defined, you can select an IF to suit your needs. In doing so, consider that certain frequencies may result in in-band intermodulation products. Tables and charts have been developed to help designers avoid these frequencies.³ Practical considerations also impose some limitations on IF selection.

The crystals used in color-burst generators at 3.579 and 4.433 MHz are the most inexpensive crystals around and are widely available as surplus components. Unfortunately, the required termination resistances of filters built with such crystals may exceed 10 k Ω , which necessitates an impedance transformation with a very high ratio (for a 50- Ω system). As a result, very high voltage levels may be developed at the filter input, which may cause an overload condition. In addition, the required values of the coupling capacitors may be under 5 pF, making construction difficult due to stray capacitances. For these reasons, crystal filters with center frequencies under 6 MHz are not recommended.

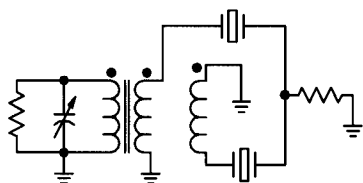
The useful upper frequency limit is determined by the influence of stray capacitances at frequencies above 10 MHz and by the limitations imposed on the VFO circuit for multiband HF operation. Consequently, the recommended frequency range for an HF SSB crystal filter is between 6 and 12 MHz. The remaining criteria for the crystal frequency selection are the crystal Q and the price. Microprocessor crystals in HC18/U or HC49/U cases are reasonably inexpensive, but, being manufactured in large quantities, they are optimized for parameters other than Q.

Q is typically not specified by the manufacturer, and it varies significantly from batch to batch and from device to device within a batch. Therefore, the only way to find the Q of a specific type of crystal is to obtain several samples and to measure the parameters. This should be done before buying a large batch of crystals.

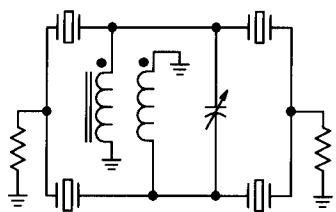
I originally intended to build crystal filters at 9 MHz, which is a popular IF within the amateur community, but it turned out that all the 9-MHz crystals I obtained (from different vendors)



A) Lattice Crystal Filter



B) Half-Lattice Crystal Filter



C) Cascaded Half-Lattice Crystal Filter

Fig 1—Lattice crystal filter circuits.

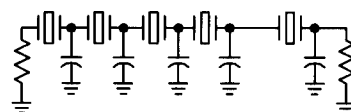


Fig 2—Circuit of a ladder crystal filter.

had Q_s below 80,000. On the other hand, I found 8-MHz crystals with much higher Q_s , so all of the crystal filters described in this article are built using 8-MHz (series resonance) crystals.

Crystal Parameters

The equivalent circuit of a quartz crystal is shown in Fig 3. The computer software we will use to design the ladder filter requires entry of the crystal parameters. These parameters are easily measured with the use of a lab-quality impedance analyzer, but they also can be measured quite accurately using home-built equipment. The test equipment required to measure crystal parameters has been described previously and is beyond the scope of this article.^{1,4,5} The parameters needed for the design process are: ΔF , the frequency offset or deviation from the specified center frequency; r , the series resistance of the crystal; f_L and f_H , the 3-dB points required for the Q calculation; and L_m , the motional inductance, which is derived from the Q and r . C_o , the parallel or "holder" capacitance, can be measured, but an assumption that C_o is 5 pF (which I verified for several crystals in HC49/U cases) appears to be adequate in most cases.

There are several practical consid-

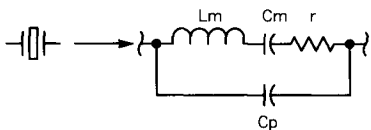


Fig 3—Equivalent circuit of a quartz crystal.

erations in selecting and handling the crystals you will use. For one thing, the design process is easier if the crystals to be used in a particular filter are selected from a large pool of crystals. Although it's not essential, the crystals can be matched for Q , L_m and ΔF . Buying a large batch of crystals may provide a volume discount and furnish you with several sets of filter crystals. To illustrate the point, I bought 100 8-MHz crystals for a total of \$60. Out of that batch I used 14 crystals with an average Q of 145,000 for a 14-pole filter, 10 crystals with an average Q of 122,000 for a 10-pole filter and 12 crystals with an average Q of 110,000 for a 12-pole filter. I rejected the remaining 64 crystals. Three high-quality crystal filters for \$60—not bad!

The crystals should be tagged before measurement, and the measurement results should be logged for future use. Invest sufficient time in this initial stage of the design since the accuracy of the data will affect the shape of the frequency response.

Take care to avoid heat transfer from your hands to the crystal cases, and allow 40 to 60 seconds between handling the crystals and performing the measurements to let the resonant frequency stabilize.

Once the measurements are completed, a preliminary group or groups of crystals with sufficiently high Q can be identified (grouped by Q within a certain range). Calculate the average motional inductance (L_{m-av}) and average Q (Q_{av}) for each group of crystals.

Filter Selection

An important part of the design process is selection of the desired filter parameters. The parameters you need

to select are:

- the filter response type—Chebyshev, Butterworth, Gaussian, etc,
- the number of poles,
- the filter bandwidth, and
- the value of terminating resistances.

The Chebyshev response with 0.1 dB of ripple is the most commonly used response type for SSB HF filters. It may be advantageous in the final filter design to deviate slightly from the 0.1-dB ripple value to obtain more convenient values for the end coupling capacitors. Decreasing the ripple level value will result in a slightly smoother frequency response but will degrade the shape factor; an increase in the ripple value causes the opposite effect.

Several factors have a significant influence on the number of poles chosen for the crystal ladder filter:

- the desired shape factor,
- the insertion loss,
- the degree of asymmetry of the frequency response,
- construction considerations, and
- the size and weight (for portable use).

The shape factor is defined as the ratio of the filter bandwidth at a level of -80 or -60 dB to its bandwidth at the -6 -dB level. In this article I'll use the $-80/-6$ dB shape factor, $SF_{6:80} = \Delta f_{-80} / \Delta f_{-6}$.

The required shape factor depends on the complexity of the receiver, its architecture and its specifications. Filters with more poles have better shape factors. (For example, the XF-9B10, a 10-pole, 9-MHz SSB filter manufactured by KVG Inc, has $SF_{6:80} = 1:1.8$.) Fig 4 may help you select the needed number of poles,

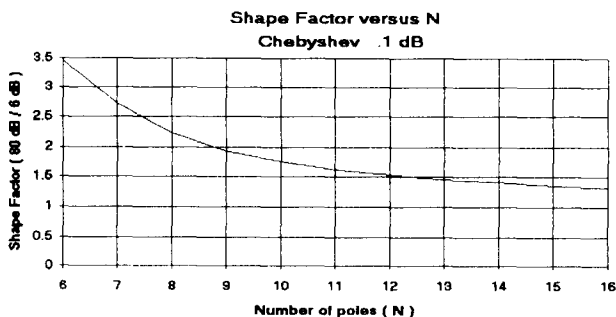


Fig 4—Graph of ladder filter shape factor (6:80) versus the number of poles for a Chebyshev response with 0.1 dB of ripple.

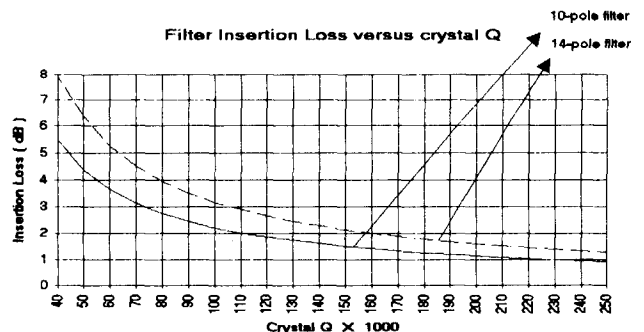


Fig 5—Graphs of filter insertion loss versus crystal Q .

based on the desired shape factor. Receivers having filters with good shape factors exhibit improved selectivity and a distinct "crisp" quality when tuning from one station to another.

Insertion loss, while strongly influenced by the Q of the crystals, also depends on the number of poles. The curves in Fig 5 show these effects. All other factors aside, the availability of good-quality crystals may be the deciding or limiting factor in selecting the number of poles. As shown in Fig 5, a 14-pole filter made of crystals having Q s of 160,000 has the same insertion loss as a 10-pole filter made of crystals having Q s of 110,000. The curves in Fig 5 were generated using *IRFD* and represent theoretical calculations performed by the program. Due to several limitations I'll discuss later, the practical results differ somewhat from the predicted values. But it is possible with a good degree of accuracy to make an estimate of the practical value of the insertion loss by adding 0.8 dB to the value obtained from Fig 5.

The asymmetry of the frequency response is inherent in crystal ladder filters, but by increasing the number of poles it is possible to overcome this shortcoming. While the asymmetry is obvious in a 10-pole filter, it becomes almost unnoticeable in a 14-pole filter.

Construction considerations will undoubtedly differ from one builder to another, but one observation is worth mentioning: I noticed during the construction of several ladder filters that to achieve good ultimate attenuation (more than 120 dB), the requirements for shielding between filter sections are considerably more stringent for a 10-pole filter than for a 12 or 14-pole filter.

Considering all the factors listed above, I recommend keeping the number of poles between 10 and 14. There is an advantage in having an even number of poles—it results in a symmetrical design, minimizing the number of different capacitor values needed.

Several factors influence the choice of bandwidth of the crystal filter:

- the desired selectivity—narrower filters may be preferred for contest work while wider filters may be more appropriate for casual rag-chewing,
- receiver sensitivity and dynamic range, and
- personal preference.

All of the filters discussed in this article have a bandwidth of 2500 Hz—mostly due to the last factor.

The value of the terminating resistance should be as low as possible to minimize the transformation ratio of the impedance-matching transform-

ers, and the value should exceed the *IRFD* recommended value by an amount that ensures that the end coupling capacitors are at least 15 pF. You should choose the lowest impedance value consistent with these two criteria from Table 1. (The transformer ratios assume you want to match the filter to 50- Ω source and load impedances.)

Computer Design

Before starting the computer design, make sure you have calculated the average Q (Q_{av}) and motional inductance (L_{m-av}) of the crystals and have selected the desired bandwidth, number of poles and the ripple value.

Note that if the actual desired bandwidth is used directly in the crystal filter design, the filter designed by the *IRFD* program will have a bandwidth narrower than predicted. (This occurs because of simplifying assumptions used in the equations and the use of k

Table 1—Termination Resistances and Transformer Design

Impedance ratio	Termination resistance (Ω)	Primary turns	Secondary turns
1:1.5	75	4	5
1:2	100	5	7
1:3	150	4	7
1:4	200	4	8
1:5	250	4	9
1:6.25	312	4	10
1:7.5	375	4	11
1:9	450	4	12
1:10.6	530	4	13
1:12.25	612	4	14
1:14	700	4	15
1:16	800	4	16

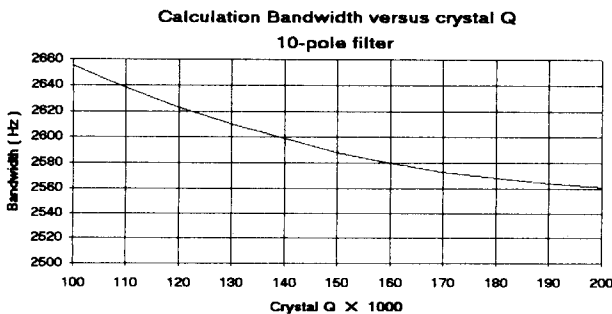


Fig 6—Graph of calculation bandwidth versus crystal Q for a 2500-Hz, 10-pole filter.

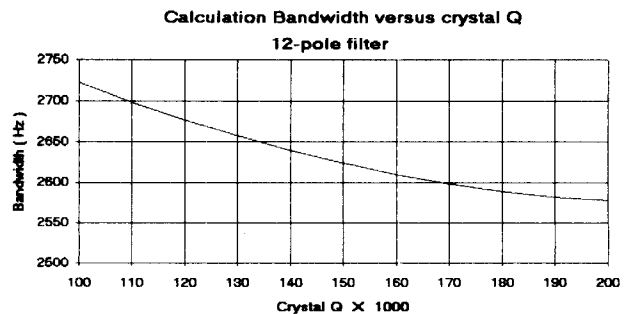


Fig 7—Graph of calculation bandwidth versus crystal Q for a 2500-Hz, 12-pole filter.

and q values based on lossless crystals.⁴) I've developed correction factors to compensate for this discrepancy. The bandwidth used for the computer calculations will be referred to as the calculation bandwidth (BW_c), which can be obtained from the charts in Figs 6 through 8 for a desired bandwidth (BW_d) of 2500 Hz.

To illustrate the design process, let's walk through the steps of an actual filter design. We'll begin by listing the design parameters:

- Number of poles (N): 12
- Desired bandwidth (BW_d): 2500 Hz
- Filter response type: Chebyshev, 0.1-dB ripple
- Crystal (Q_{av}): 110,000
- Motional inductance (L_{m-av}): 0.0155 H
- Parallel capacitance (C_o): 5 pF
- Nominal crystal frequency: 8 MHz

Four programs from the *IRFD* software package will be used to accomplish the design: *GPLA*, the general purpose ladder analysis program; *L*, the low-pass filter design program; *X*, the ladder crystal filter design program; and *MESHTUNE*, a utility for tuning meshes in a crystal filter. In each program, the menu selections are selected by typing the appropriate letter key. Entry of numeric values is done by typing the value, then pressing the **Enter** key. (See the *IRFD2MAN.TXT* file supplied with *IRFD* for details of program operation.)

To start the design process, use the *L* program to generate k and q values for the filter. Run *L*, then select **K** from the menu. Type **12** for the number of poles, then **0.1** for the ripple, in dB. (The program calculates the needed values and stores them in a disk file for the *X* program to use.) Press the **Enter** key until the *L* program exits.

Next, run the *X* program to perform the ladder filter design. Select **K** from the menu to load the k and q values from the disk file. Type **12** for the number of meshes, **8** for the nominal crystal frequency, **0.0155** for the motional inductance in henries, **1** for the overtone, **5** for the parallel capacitance in pF (assumed), and **110** for the crystal Q in thousands. *X* now wants you to enter the k and q values. Since they are on disk, you can just press the **Enter** key repeatedly to load the data generated by the *L* program, until *X* stops asking for the values and instead asks for the bandwidth in hertz. The bandwidth you enter, **2700**, is the bandwidth obtained from the chart in Fig 7, for a 12-pole filter with a desired bandwidth of 2500 Hz. Press **Enter** to get to the source termination resistance prompt. Although the end resistance value given by the *X* program in this step is 206 Ω , an attempt to use the 250 Ω given in Table 1 fails—the actual minimum possible termination is 274 Ω . But the use of that termination value would make for very small (2.2 pF) end coupling capacitors, so the next highest termination value is selected from Table 1. Enter **312**. *X* will next ask for the termination value for the load end of the filter. Just press **Enter**, as 312 is now the default. At this point the values of the coupling capacitors are displayed on the screen. You can print a hard copy by using your computer's print-screen key. The values of all the capacitors are practical and can be easily realized with either a single capacitor or two capacitors in parallel. The values of the coupling capacitors will not be altered during the alignment stage and should be considered final. Pressing **Enter** displays the second set of data vital to the design: the mesh offset frequen-

cies. You should print this screen as well, as this data will be used later in the design procedure. Another **Enter** displays the menu. It's useful at this point to closely examine the coupling capacitor values. If they appear satisfactory, you are done with this stage of the design and can save the designed filter to disk by pressing the **D** key. If you want to change the design, you can alter the termination resistances with the **R** key or change the calculation bandwidth with the **W** key.

Altering the termination resistances affects only the values of the end coupling capacitors; it is easy to vary these values and see the effect, so feel free to experiment. Altering the bandwidth affects all of the coupling capacitors. You shouldn't change the bandwidth by more than about 30 Hz from the initial value since it will invalidate the later stages of the design procedure.

Changing the ripple value is another option, but the design will have to be repeated from scratch since the k and q values have to be changed by the *L* program. Possible values for the filter ripple may be between 0.07 and 0.15 dB.

Be sure to store the final design in a file using the **D** key. For this example, we'll call the file **12POL1**. (The *X* program will automatically add **.CIR** to the end of the file name.) The stored file can be viewed or edited with a text editor. Make a hard copy of the file for future reference.

We can investigate the response of the filter we've designed using the *GPLA* program. If you have a VGA display, *GPLA* can plot the frequency response of your screen. Run *GPLA* and read in the saved circuit using the **R** key. Once the file has been read in, press the **P** key to select plotting, then press the **H** key to get the filter gain plot. The filter response should be displayed. After viewing the plot, press the **Esc** key to return to the menu. To find the theoretical insertion loss of the filter, we need to adjust the sweep parameters to get a close-in look at the pass-band response. Press **S** to set up the sweep, type **400** for the beginning frequency, **3500** for the end frequency, **30** for the frequency step, **310** for the grid spacing, **10** for the screen bottom, and **1** for the dB/division. Then press **P** followed by **H**. The theoretical insertion loss of the filter is the distance from the top of the plot to the highest point on the response curve, at 1 dB per division. The loss appears to be

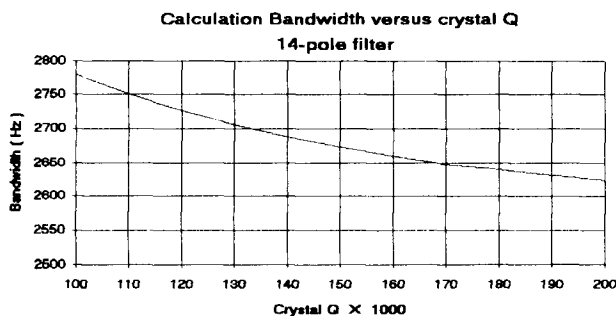


Fig 8—Graph of calculation bandwidth versus crystal Q for a 2500-Hz, 14-pole filter.

slightly over 2 dB. A practical value for the loss may be estimated by adding 0.8 dB to the theoretical loss, for a result of about 3 dB. To exit this screen press **Esc**.

If crystal resonators with frequency offsets equal to the mesh offset frequencies listed by the X program were available, the computer design would be finished at this point. Since that's unlikely, additional steps are required in order to tune the crystals to the required offset frequencies, making the use of crystals with random (but known) offset frequencies possible.

To accomplish this, tuning capacitors are inserted in series with the crystals. These capacitors allow considerable design flexibility and tune every crystal to the same "loop frequency."^{1,4} This modification results in the schematic diagram shown in Fig 9.

Our next step is to "build" this new filter circuit for analysis using a utility program and the *IRFD* software. We will do this by creating a modified copy of the 12POL1.CIR circuit file.

Our new circuit file adds series tuning capacitances to the circuit and changes the original crystal offset frequencies calculated by the X program to the actual measured offset frequencies (ΔF) of the crystals we will use in the filter. All of the values we need to deal with are shown in Table 2.

If you investigate the coupling capacitor values and the mesh offset frequencies shown in Table 2 (or on your hard copy from the X program), you'll find that the values are symmetrical around the middle. Although it's not essential, it is helpful to arrange the crystals in pairs in an attempt to preserve the symmetry. Columns A and B in Table 2 help to illustrate the arrangement. The two crystals with the highest positive frequency offset are placed at the edges (X2 and X35). The two crystals with the highest negative frequency offset are placed next (X5 and X32). The remaining crystals are arranged monotonically and symmetrically around the middle.

The *CLFMOD* program (see Listing 1) is a simple utility program written

in BASIC by Jon Bloom, KE3Z, of ARRL HQ.⁶ It reads the original filter circuit file output by the X program and writes the modified circuit file we will work with (call it 12POL2.CIR). This file adds the tuning capacitors to the original filter circuit, setting the value of each tuning capacitor to 200 pF. It will ask you to enter the measured frequency offsets of the crystals, as shown in column B of Table 2, and it will calculate and display the combined offset shown in column D of Table 2. These values will also be written to the *OFFSETS.CLF* file. (It's helpful to make a table like Table 2 so you don't get lost.) Note that if you arranged the crystals as recommended, the spread of the offset frequencies in the middle of column D is minimized, which leads to a narrow spread of the eventual tuning capacitor values, as shown in column F. (The coupling capacitor values obtained earlier are presented in column J.)

Now the values of the tuning capacitors should be calculated and entered into the circuit. We will use the

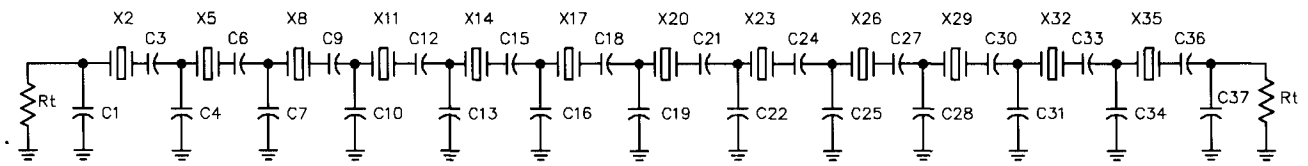


Fig 9—Schematic diagram of the example 12-pole crystal filter.

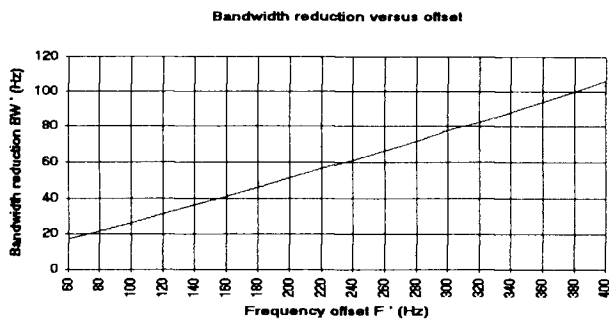


Fig 10—Bandwidth-reduction graph. The needed frequency offset can be obtained once the desired bandwidth reduction is found.

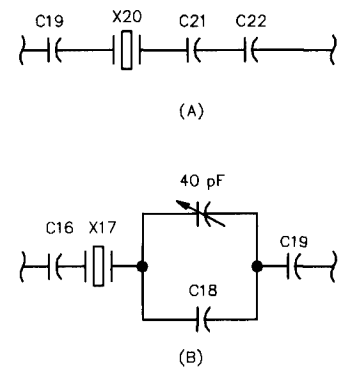


Fig 11—Filter alignment circuits. The resonant frequency of the reference loop is measured using the circuit at A. For the other loops, the required tuning capacitance is found by adjusting the variable capacitor at B to get the same resonant frequency.

MESHTUNE program to find the required tuning capacitor values. Run **MESHTUNE** and press **B** to start a new mesh. Type **8** for the nominal crystal frequency and press **Enter** for the crystal offset frequency. (Do *not* enter an offset frequency!) Type **0.0155** for the motional inductance and **0** for the crystal parallel capacitance. Press **Enter** to get to the interior/exterior prompt, then press **I**. Enter **1000000000** (1 followed by 10 zeroes) for the left-hand coupling capacitor and the same value for the right-hand coupling capacitor. Enter **300** for the initial value for the tuning capacitor. For the target offset frequency, enter the target offset frequency calculated by **CLFMOD** for this mesh (column D of Table 2). The actual mesh offset frequency and the target offset frequency will be displayed. Note whether the mesh is tuned too low or too high. (It's too low in this case.) Press **Enter** to get back to the menu. If the mesh was tuned too low, press the down arrow key to reduce the tuning capacitor; if the mesh is tuned high, press the up arrow key instead. The new tuning capacitor value will be displayed, as will the target and new actual mesh frequencies. Continue pressing the same key until the mesh frequency crosses over the target frequency.

To fine-tune the capacitor value, press the **S** key to set the tuning capacitor step. Enter **0.1** for the step size. Now, using the arrow keys, tune back across the target frequency until it again changes from too high to too low, or vice versa. At the point where

it changes, the displayed tuning capacitor value will be within 0.1 pF of the perfect value—close enough! Enter the final capacitor value into column F of the table.

To obtain the next tuning capacitor value, start over by pressing **B**. Note now that most of the values you entered previously default to the correct numbers, so you can just press **Enter** for those parameters. Remember to enter the correct target offset frequency for the crystal you are tuning. Repeat the tuning process. For some crystals, the required value of tuning capacitance may be quite large. In such cases, you may want to increase the tuning step size using the **S** command. It's easy to watch the actual mesh frequency as you tune and get a feel for whether you need to raise or lower the step size for effective tuning.

The above tuning procedure may seem cumbersome, but once you get the hang of it, things go pretty quickly.

We now need to create the final filter circuit file so we can check its response using **GPLA**. Use a text editor such as **DOS EDIT** or **Windows Notepad** to open the **12POL2.CIR** file. Each tuning capacitor entry consists of three lines:

```
cap <ref>
ser
200
```

where <ref> is the reference designator of the component (e.g., C3). For each tuning capacitor, C3, C6,...C36, change the line reading 200 to the value for that capacitor from column F of Table 2. For C3, the result is:

```
cap c3
ser
279.8
```

Do not change any of the other lines in the file. When all of the tuning capacitor values have been changed, save the file as **12POL3.CIR**.

Next, run **GPLA** and press **R** to read in the **12POL3.CIR** file. Then press **S** to set up the sweeps for a beginning frequency of **0**, an end frequency of **4000** a frequency step of **40**, a frequency grid spacing of **200**, a screen bottom of **10** and **1** dB per division. Then press **P** followed by **H** to see the filter response curve. Make an estimate of the insertion loss in the middle of the pass-band. Press **Esc** to return to the menu.

Determine the -3 dB points by changing the sweep settings to make the bottom of the screen 3 dB below the insertion loss. The insertion loss in this example is about 2.3 dB, so set the bottom to 2.3 + 3 = 5.3. When you redisplay the gain plot, the -3 dB level will be at the bottom of the screen, and a rough estimate of the bandwidth can be done by determining the two points at which the filter response curve meets the bottom of the chart. A more accurate estimate can be performed by modifying the sweep such that the gain curve originates at the beginning of the sweep interval and finishes at the end of the sweep interval. This sweep modification may require several tries to get it just right. In this example, you should end up with a sweep range of about 520 to 3225. The -3-dB bandwidth can be easily calcu-

Table 2—Design Parameters for the Example 12-Pole Filter

A	B	C	D	E	F	G	H	I	J
Crystal #	Crystal offset (Hz)	Mesh offset (Hz)	Combined offset (Hz)	C#	Tuning capacitor (pF)	New offset (Hz)	New tuning capacitor (pF)	C#	Coupling capacitor (pF)
2	+17	381.99	364.99	3	279.8	534.99	190.9	1	23.84
5	-67	0	67.0	6	1524	237	431.0	4	77.20
8	-60	320.66	380.66	9	268.3	550.66	185.5	7	103.26
11	-55	383.96	438.96	12	232.7	608.96	167.7	10	109.54
14	-15	405.96	420.96	15	242.6	590.96	172.8	13	111.79
17	-4	413.86	417.86	18	244.4	587.86	173.7	16	112.70
20	0	413.86	413.86	21	246.8	583.86	174.9	19	112.95
23	-9	405.96	414.96	24	246.1	584.96	174.6	22	112.70
26	-34	383.96	417.96	27	244.4	587.96	173.7	25	111.79
29	-55	320.66	375.66	30	271.9	545.66	187.2	28	109.54
32	-61	0	61.0	33	1674	231	442.1	31	103.26
35	+26	381.99	355.99	36	286.9	525.99	194.2	34	77.20
								37	23.84

lated: $BW_3 = 3225 - 520 = 2705$ Hz.

This bandwidth is too high for the final design, but that was done intentionally. The final step in the computer design involves adding an additional frequency offset to reduce the bandwidth to a predetermined value. The purpose of this procedure is twofold: first, it reduces the value of the tuning capacitors, making it more practical to use two parallel capacitors; second, it further narrows the range of capacitor values (see column H of Table 2), possibly minimizing the number of required capacitor values.

The target bandwidth for the computer design is 6.5% higher than the desired bandwidth: $BW_t = 1.065 \times BW_d = 1.065 \times 2500 = 2662$ Hz.

The bandwidth reduction: $BW' = BW_3 - BW_t = 2705 - 2662 = 43$ Hz. The additional frequency offset required to accomplish this bandwidth reduction can be obtained from Fig 10. From the chart, a 43-Hz reduction requires an additional frequency offset, $F' = 170$ Hz. Offset F' is added to the value of the combined offset in column D of Table 2, and the new value is entered in column G. (The *CLFOFS* program, included with the *CLFMOD* program, can be used to perform these calculations.) By using the *MESHTUNE* program and the tuning procedure described earlier new values for the tuning capacitors are obtained and entered in column H of Table 2. File 12POL3.CIR should be modified one more time to include the updated capacitor values and saved as 12POL4.CIR.

Finally, the filter bandwidth should be checked again. If the -3 dB bandwidth (BW_3) is within 15 Hz of the target bandwidth ($BW_t = 2662$ Hz), the computer design is completed. Other-

wise modify the value of offset F' using the chart in Fig 10 as a guideline and calculate new tuning capacitor values to obtain the required target bandwidth.

Construction and Alignment

The construction method described in this section is an alternative to a printed-circuit board. The filter components are mounted on a piece of Vector board (Vector part no. 8007). The crystals, matching transformers and the attenuator are mounted on the copper side, which is used as a ground plane. All ground connections are made directly to the ground plane. The capacitors and the intersection shields are mounted on the pad side of the board. The interface with other stages is done through BNC connectors which can be soldered directly to the board, or via coaxial cables which can be soldered to Vector pins (Vector part no. T44). Photo 1 shows the filter assembly.

The construction involves several steps. In the first step, only the crystals are mounted on the board. The crystals identified previously should be arranged on the board in the sequence determined in column A of Table 2. The separation between the leads of adjacent crystals is 0.2". The leads should be soldered to the pads while making sure that the crystals are mounted firmly against the ground plane. I do not recommend you ground each crystal case via a wire ground strap; the risk of altering the crystal parameters during soldering is too great to take. The crystal leads should be clipped to $\frac{1}{8}$ inch. It is helpful at this point to label the crystals on the pad side of the board for easy identification.

The second step is the formation of the coupling capacitances (see column J of Table 2). These are formed by paralleling capacitors, taking into account the approximately 3 pF of stray capacitance present:

C1, C37: 10 pF + 10 pF (+ 3.84 pF of stray capacitance)

C4, C34: 47 pF + 27 pF (+ 3.20 pF of stray capacitance)

C7, C31: 100 pF (+ 3.26 pF of stray capacitance)

C10, C28: 68 pF + 39 pF (+ 2.54 pF of stray capacitance)

C13, C25: 82 pF + 27 pF (+ 2.79 pF of stray capacitance)

C16, C22: 100 pF + 10 pF (+ 2.70 pF of stray capacitance)

C19: 100 pF + 10 pF (+ 2.85 pF of stray capacitance)

The selection process is greatly facilitated if the capacitors are picked from a 5% or 10% stock using a capacitance meter with at least 0.1-pF resolution. The parallel combinations of the selected capacitors should be formed by soldering them together and trimming the leads to $\frac{3}{16}$ inch. The capacitors should then be tagged with their component number for easy identification.

To complete the design, the final values of the tuning capacitors must be determined. The values calculated in column H of Table 2 are preliminary but indicative of the capacitance range required for tuning. The tuning procedure is based on the fact, from filter theory, that each loop in the ladder filter should be resonant at the same frequency.^{1,4} In other words, each crystal-and-tuning-capacitor combination, when put in series with the coupling capacitors on each side of it, should resonate at the same loop frequency.

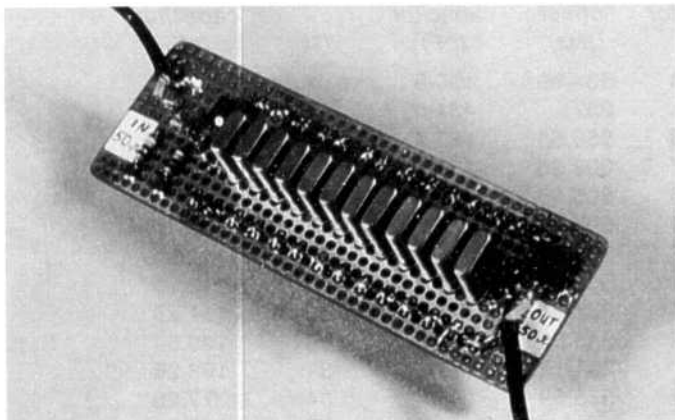


Photo 1

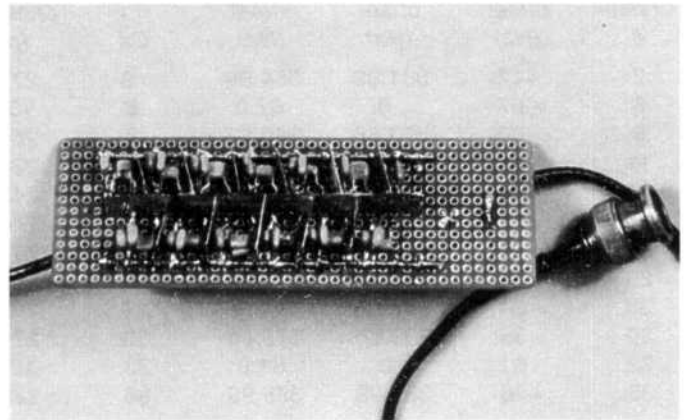


Photo 2

To find a starting point, refer to column H of Table 2. A convenient value from the middle of the column is selected: $C_{21} = 174.93 \text{ pF} = 150 \text{ pF} + 22 \text{ pF}$ (+ 2.93 pF of stray capacitance). Connect this parallel combination of two capacitors in series with crystal X20 (see Fig 9) and the two coupling capacitors on either side of the crystal, C19 and C22, as shown in Fig 11A. The series-resonant frequency of this circuit can be found with the aid of a crystal tester. This becomes the loop frequency, and all remaining loops have to be tuned to this frequency. Note that the predicted values of the tuning capacitors in the center section of the filter vary within a narrow range.

To determine the value of the next tuning capacitor, connect a parallel combination of a 150-pF capacitor and a 40-pF variable capacitor in series with crystal X17 (see Fig 10) and the two coupling capacitors on either side of the crystal, C16 and C19 (see Fig 11B). Use the crystal tester to measure the resonant frequency of this series combination, tuning the variable capacitor until the circuit is resonant at the loop frequency. The proper value for C18 is then found by measuring the value of the parallel combination of the 150-pF capacitor and the variable capacitor. Form this capacitance using paralleled fixed-value capacitors and tag it as C18. This procedure is repeated for all of the tuning capacitors except those at either end of the filter. During this procedure, each coupling capacitor is used twice: once while selecting a tuning capacitor on its left and again while selecting a tuning capacitor on its right.

The procedure for determining the values of the tuning capacitors at the ends of the filter differs only slightly: A 316- Ω resistor (the termination resistance) is placed across the end coupling capacitor, C1, when determining the value of C3 and across capacitor C37 when determining the value of C36. The terminating resistors lower the Q of the circuit, so the tuning of C3 and C36 is not very critical. Remember that when you perform filter measurements the scope probe capacitance (approximately 10 pF) and the generator output capacitance (approximately 5 pF) will be added to the respective terminals. Therefore, after the tuning process has been accomplished the values of capacitors C1 and C37 have to be modified to compensate for the source and load capacitances.

Once the values of all of the tuning capacitors have been determined, filter construction can continue. Construct the ground bars and mount them on the pad side of the board before installing the capacitors. Each ground bar is made from #16 copper wire (stripped of insulation), cut to a length of $[(0.2 \times N) + 0.5]$ inches, where N is the number of crystals. Place each ground bar symmetrically, 0.35-inch away from the pins of the crystals (see Fig 12) and solder it to the ground plane every 0.2 inch (every other hole) using jumpers made out of small-diameter hook-up wire. Next, solder the tuning capacitors in place following the placement diagram shown in Fig 12. Take care not to overheat the crystals during soldering. The load coupling capacitor, C37, and tuning capacitor, C36, are soldered to a Vector pin.

Install the coupling capacitors following the diagram of Fig 12. While the tuning capacitors are mounted horizontally, the coupling capacitors are placed vertically to conserve space. Make the capacitor leads as short as practical, keeping in mind that longer leads can cause excessive crosstalk between sections, and very short leads can lead to capacitor cracking during the soldering process. Provide sufficient clearance between adjacent sections to accommodate the shield ribs. These are made from $\frac{3}{8}$ -inch-wide strips of metal. Brass, copper or tinned 0.02-inch steel will do, providing it can be easily soldered to the ground plane. The shield is arranged in a "fish-bone" fashion. The center section is cut to a length of $[(0.2 \times N) + \frac{3}{16}]$ inches and is

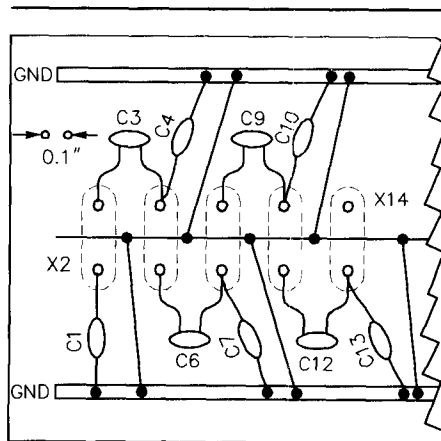


Fig 12—Layout diagram of the crystal filter.

placed vertically exactly in the middle between the pins of the crystals (see Photo 2). Keep it in place by soldering it to Γ shaped posts. These are made from #18 copper wire (stripped of insulation), with the short end soldered to the ground plane. Insert the intersection ribs between adjacent sections of the filter and solder them to the center rib on one side (at the top only) and to the ground bars on the other side. More comprehensive shielding can be accomplished by fully encapsulating the filter components in a metal enclosure, but I've obtained adequate performance without this precaution.

Matching transformers are used to present a 50- Ω input and output impedance to the outside world. The winding information is taken from Table 1. The transformers are wound with #32 enameled wire on two-hole ferrite balun cores (see Fig 13). In Table 1, "primary turns" refers to the number of turns from the tap to ground, and "secondary turns" refers to the number of turns of the entire winding. Mount both transformers on the ground-plane side of the board in close proximity to the crystals. Solder the tap leads to Vector pins on the ground-plane side of the board. The Vector pin on the input side is also connected to the output of a 3-dB attenuator (see Fig 14). Place the attenuator components on the ground-plane side of the board as well, making the connections on the pad side. Then con-

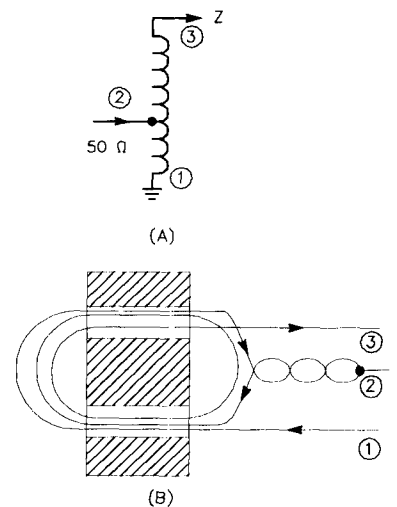


Fig 13—The matching transformers are tapped autotransformers (A), wound as shown at B.

nect the attenuator input to another Vector pin, which serves as the filter input terminal. The board area taken by the entire 12-pole filter circuit is $3\frac{3}{4} \times 1\frac{1}{8}$ inches.

Measurements

Now that the filter is finished, we need to measure its response, which should match the design objectives: shape of the response, -3 dB points, bandwidth, amount of ripple, insertion loss and the symmetry of the response. Making the measurements is a trivial task when a spectrum analyzer is at hand, or at least a good synthesized generator and a scope. Since few amateurs have the luxury of using lab-quality equipment, I suggest a simple method that should be within reach of the average experimenter. It requires the construction of a variable-frequency crystal oscillator (VXO). The VXO should tune from 8.000 MHz to at least 8.005 MHz. (One of the rejected filter crystals can be used in the VXO—use the one with the most negative offset.) The VXO should have a level adjustment control and adequate buffering at the output to prevent frequency pulling when being loaded by

the crystal filter. Many variations of VXO design have been covered in the amateur literature.^{4,7,8,9,10} A frequency counter with 1-Hz resolution and an oscilloscope are also needed to perform the measurement.

The block diagram of the measurement setup is presented in Fig 15. The measurement procedure is to vary the frequency of the VXO in small increments (20 to 80 Hz) while monitoring and recording the signal level at the output of the filter at each frequency. Hold the VXO output level constant at every measurement point.

I used lab-quality test equipment (a Hewlett-Packard HP3585A spectrum analyzer) to measure three ladder filters—10-pole, 12-pole and 14-pole designed and constructed using the procedures outlined in this article. The measured response curves of these filters are shown in Fig 17, with the ripple level for the 14-pole filter shown in Fig 18. The measured bandwidth of all three filters is within 2% of the desired bandwidth, and the shape factor is within 3% of the calculated value. The ripple level is slightly higher than the projected value but significantly better than several commercial units I tested.

To compare the performance of my home-built ladder filters to that of commercially available crystal filters, I made a series of measurements using laboratory-grade measurement equipment. The block diagram of the measurement setup is given in Fig 16. The amplifier used in the measurement has an output third-order inter-

cept point (OIP) of $+48$ dBm and a -1 dB output compression point of $+27$ dBm. One of my objectives was to study each crystal filter's dynamic range and its effect on the output intercept point of the driving amplifier.

Four crystal filters have been evaluated: a 2.2-kHz, 8-pole SSB filter from Fox-Tango Corp (part no. 2309) and the three home-built ladder filters mentioned previously. The Fox-Tango filter requires a 500- Ω impedance termination, so it was coupled to the amplifier via a 1:9 transformer. The test results were very similar for all three ladder filters, so they will be referred to collectively as the "ladder crystal filter."

The input impedance of the filters was examined using an HP impedance analyzer and re-examined after inserting an attenuator between the amplifier and the crystal filter. For the ladder filter, a 3-dB attenuator was used; a 6-dB attenuator was used with the Fox-Tango filter. Figs 19 through 22 show the results of these measurements.

To measure the IMD of the filters, I used two equal-level tones placed outside of the filter pass-band. The tone spacing was varied between 2 and 20 kHz without an appreciable effect on the third-order products measured at the output of the amplifier. These measurements were made at two different signal levels ($+15$ dBm and $+10$ dBm) in order to gauge the linearity of the system. The measurements were made while driving the filter directly by the amplifier and again

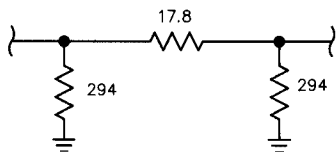


Fig 14—Schematic diagram of the 3-dB input attenuator used with the ladder filter.

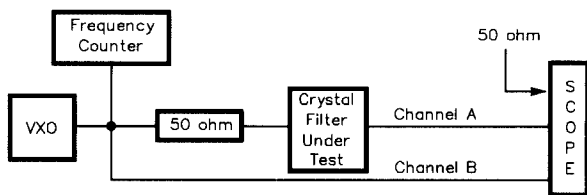


Fig 15—Block diagram of the filter evaluation test set-up.

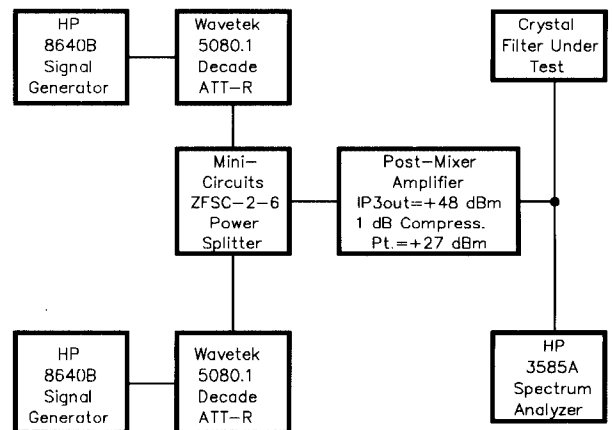
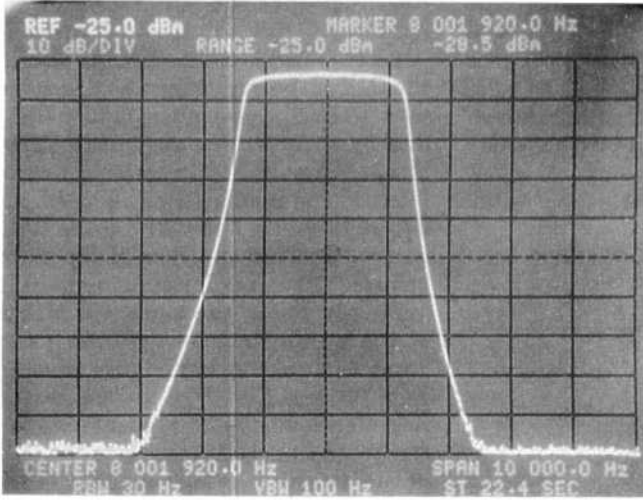
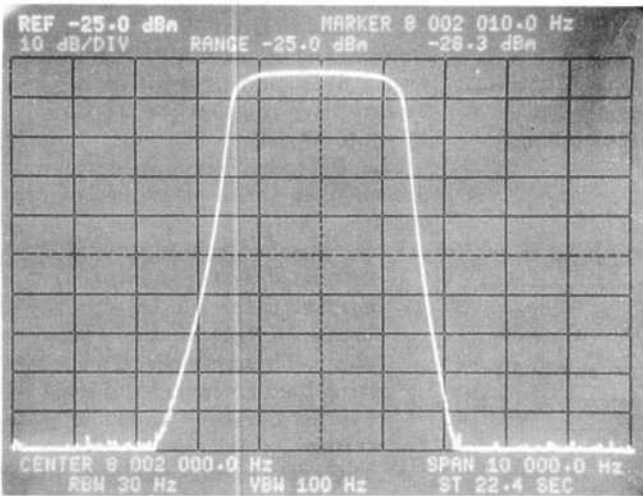


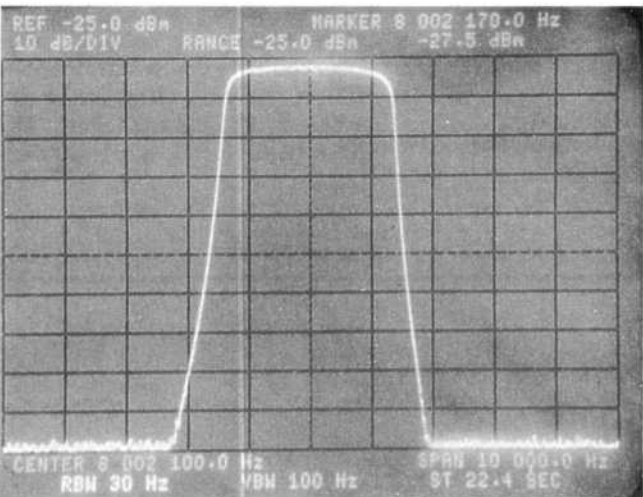
Fig 16—Block diagram of the filter IMD measurement test set-up.



(A)



(B)



(C)

Fig 17—The measured response of a 10-pole (A), 12-pole (B) and 14-pole (C) ladder filter built using the techniques described by the author. Vertical divisions are 10 dB; horizontal divisions are 1 kHz.

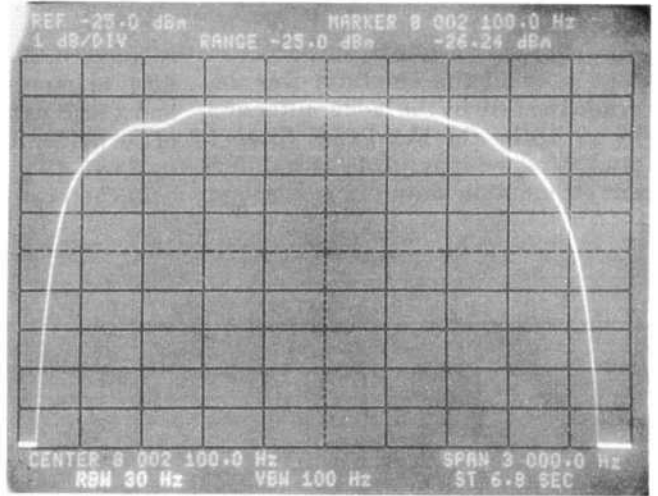


Fig 18—A close-in look at the response of the 14-pole ladder filter shows the pass-band ripple. Vertical divisions are 1 dB; horizontal divisions are 300 Hz.

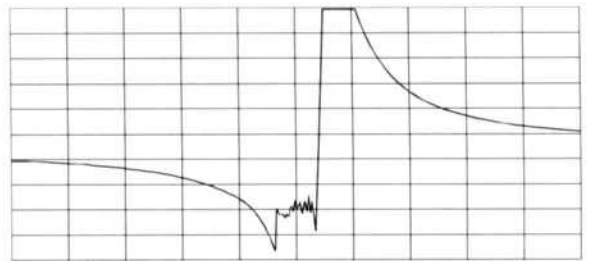


Fig 19—The measured impedance of a 14-pole crystal ladder filter. The vertical divisions are 20 Ω , with zero at the bottom. The horizontal divisions are 4 kHz each.

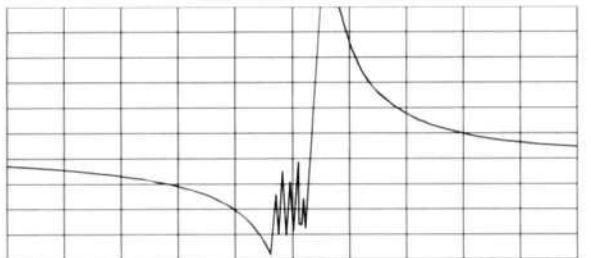


Fig 20—The measured impedance of a Fox-Tango crystal lattice filter. The vertical divisions are 20 Ω , with zero at the bottom. The horizontal divisions are 4 kHz each.

while driving the filter through a resistive pad. The measurement results are given in Table 3. The output intercept point of the amplifier was degraded by 5 dB by the ladder filter and by 12 dB by the Fox-Tango filter. I tried using resistive pads with different attenuation values in an attempt

to “smooth out” the impedance presented to the amplifier. A 6-dB pad is required in the case of the Fox-Tango filter to improve the OIP by 5 to 6 dB, and a 3-dB pad is sufficient in the case of the ladder filter to improve the OIP by 3 to 5 dB.

In the next experiment, one of the

tones was placed in the center of the pass-band and the second tone was –20 kHz away. In this measurement, the OIP of the amplifier was degraded by 4 dB in the case of the ladder filter and by 11 dB in the case of the Fox-Tango filter. A 3-dB resistive pad in front of the ladder filter reduced the degradation by 1 to 3 dB, and a 6-dB pad in front of the Fox-Tango filter reduced the degradation by 6 to 7 dB.

Finally, one of the tones was placed at the leading edge of the filter pass-band (notice the impedance dips in Figs 19 and 20). Due to the severe impedance mismatch presented to the two tones at both frequencies the OIP of the amplifier is degraded by 11 dB in the case of the ladder filter and by 22 dB in the case of the Fox-Tango filter. Resistive pads have a profound effect on the performance in this case: a 3-dB pad in front of the ladder filter reduces the degradation by up to 17 dB!

The following conclusions can be drawn from these measurement results:

- Because of the highly reactive nature of its input impedance, a crystal filter has a significant loading effect on the preceding stage. This may become the limiting factor when calculating the overall dynamic range of a receiver.
- The experiments suggest that it is more meaningful to evaluate the effect of the filter on the preceding stage than to attempt to measure the OIP of the crystal filter itself.
- Some non-linear behavior was observed (the degradation of the OIP of the preceding stage depends on the signal level). The filter behavior is more predict-

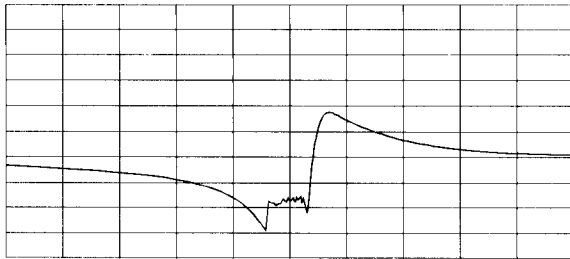


Fig 21—The measured impedance of a 14-pole crystal ladder filter with a 3-dB attenuator at the input. The vertical divisions are 20 Ω , with zero at the bottom. The horizontal divisions are 4 kHz each.

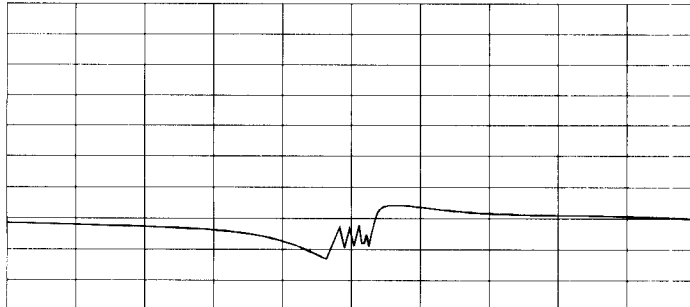


Fig 22—The measured impedance of a Fox-Tango crystal lattice filter with a 6-dB attenuator at the input. The vertical divisions are 20 Ω , with zero at the bottom. The horizontal divisions are 4 kHz each.

Table 3—Measurement results

Third-order output intercept point of the amplifier (+dBm)

Tone location relative to the passband	Ladder filter		Fox-Tango filter		Tone level (+dBm)
	No pad	3-dB pad	No pad	6-dB pad	
Both tones outside of passband	45	47	38	43	15
One tone inside of passband	44	46	37	44	15
One tone at the edge of passband	38	42	30	43	15
	43	45	36	42	10
	45	46	37	43	10
	37	42	26	43	10

Listing 1

Page 1: BASIC

```
' Modify IRFD circuit files contining crystal-ladder filters
' to add tuning capacitors for offset crystal frequencies.
,
' From "Designing and Building High-Performance Crystal Ladder
' Filters," QEX, January, 1995
,
' J. Bloom, KE3Z
' 12/08/94
,
' Note: Little checking of the input file is performed. Only files
' written by the IRFD program "X" should be used as input files.

CLS
PRINT "CLFMOD -- Modifies IRFD ladder crystal filter circuit files for tuning"
PRINT
INPUT "Enter name of original circuit file: ", f1$
OPEN f1$ FOR INPUT AS #1
INPUT "Enter name of output circuit file: ", f2$
OPEN f2$ FOR OUTPUT AS #2
OPEN "OFFSETS.CLF" FOR OUTPUT AS #3
' Get the number of circuit elements
INPUT #1, x
N = (x - 2) / 2      ' Number of poles
' Write the new number of circuit elements, including tuning caps
PRINT #2, N * 3 + 2
' Copy the unchanging parameters
FOR i = 1 TO 14
    INPUT #1, x
    PRINT #2, x
NEXT i
' Loop through each of the meshes, annotating the elements with
' component designators as in Fig 9, adding the tuning capacitors,
' and replacing the crystal offset frequencies with those of the
' real crystals.
FOR i = 0 TO N - 1
    ' Coupling capacitor
    INPUT #1, x$
    PRINT #2, x$, LEFT$(x$, 1) + MID$(STR$(i * 3 + 1), 2)
    INPUT #1, x$
    PRINT #2, x$
    INPUT #1, x
    PRINT #2, x
    ' Crystal
    INPUT #1, x$
    y$ = LEFT$(x$, 1) + MID$(STR$(i * 3 + 2), 2)
    PRINT #2, x$, y$
    INPUT #1, x$
    PRINT #2, x$
    INPUT #1, x
    PRINT "Crystal"; i + 1; "("; y$;
    INPUT ") delta F: ", y
    PRINT #2, y
    PRINT "Target offset frequency for mesh"; i + 1; "= "; x - y
    PRINT #3, x - y
```

Listing 1 (continued)

Page 2: BASIC

```
' Tuning capacitor
PRINT #2, "cap", "c" + MID$(STR$(i * 3 + 3), 2)
PRINT #2, "ser"
PRINT #2, 200
NEXT i
' Load end coupling capacitor
INPUT #1, x$
PRINT #2, x$, LEFT$(x$, 1) + MID$(STR$(N * 3 + 1), 2)
INPUT #1, x$
PRINT #2, x$
INPUT #1, x
PRINT #2, x
' Should only be one line left, but "just in case," copy to
' end of file
WHILE NOT EOF(1)
    LINE INPUT #1, x$
    PRINT #2, x$
WEND
' Clean up and exit
CLOSE
SYSTEM

' CLFOFS -- Generates final offsets for ladder crystal filter design
'
' From "Designing and Building High-Performance Crystal Ladder
' Filters," QEX, January, 1995
'
' J. Bloom, KE3Z
' 12/08/94

CLS
PRINT "CLFOFS -- Calculates final design offsets for ladder crystal filters"
PRINT
INPUT "Frequency offset for bandwidth reduction: ", f
OPEN "OFFSETS.CLF" FOR INPUT AS #1
WHILE NOT EOF(1)
    INPUT #1, x
    PRINT x + f
WEND
CLOSE
SYSTEM
```

able at the flat portions of the frequency response and less predictable when extreme impedance changes are encountered. Resistive pads tend to improve the linearity.

- If no resistive pad is used, the degradation of the amplifier's OIP is reduced by at least 7 dB if

the Fox-Tango filter is replaced by a ladder filter.

- A 6-dB resistive pad is required to significantly reduce the degradation of the amplifier's OIP in the case of the Fox-Tango filter. A 3-dB pad is sufficient to produce the same effect in the case of the ladder filter.

- The level of the third-order products at the output of the Fox-Tango filter deviates from the calculated value by more than 6 dB, even with a 6-dB resistive pad. In the case of the ladder filter, this deviation is reduced to a value under 1 dB if a 3-dB resistive pad is employed.

- Examination of the plot of input impedance of the two types of filters (Figs 19 and 20) reveals that the ladder filter has a much smoother response in the pass-band. This must be one of the reasons for the ladder filter's superior performance.

Summary

I've shown that home construction of high-performance crystal filters is quite practical, and that laboratory-grade equipment, although helpful, is not required. Home-built ladder filters can exhibit performance superior to that of commercially available filters at reasonable cost. The design and construction procedure outlined above enables the amateur to tailor the frequency response of the filter to fit the needs of the project.

Acknowledgments

I wish to express my appreciation to Wes Hayward, W7ZOI, Bill Carver, K6OLG/7, Colin Horrabin, G3SBI and Peter Chadwick, G3RZP for the helpful discussions that enabled me to better understand this subject and the encouragement to pursue this project.

Notes

¹Carver, B., K6OLG/7, "High-Performance Crystal Filter Design," *Communications Quarterly*, Winter 1993, pp 11-18.

²Hayward, W., W7ZOI, *Introduction to Radio Frequency Design*, ARRL, Newington, Connecticut, 1994, chapters 2 and 3.

³Drentea, C., WB3JZO, *Radio Communications Receivers*, Tab Books Inc, Blue Ridge Summit, 1982, pp 69-75.

⁴Hayward, W., W7ZOI, "A Unified Approach to the Design of Crystal Ladder Filters," *QST*, May 1982, pp 21-27.

⁵DeMaw, D., W1FB, "A Tester for Crystal F, Q and R", *QST*, January 1990, p 21.

⁶The source code and executable versions of *CLFMOD* and *CLFOFS* are in the *QEXCLF.ZIP* file, available for download from the ARRL BBS (203-666-0578) or via the Internet by anonymous FTP to ftp.cs.buffalo.edu, in the /pub/ham-radio directory.

⁷Hayward, W., W7ZOI and DeMaw, D., W1FB, *Solid State Design for the Radio Amateur*, ARRL, Newington, Connecticut, 1977, p 171.

⁸*The ARRL 1986 Handbook*, ARRL, Newington, Connecticut, 1985, p 10-3.

⁹Noble, F., W3MT, "A Variable Frequency Crystal Oscillator," *QST*, March 1981, pp 34-37.

¹⁰DeMaw, D., W1FB, "Some Practical Aspects of VXO Design", *QST*, May 1972, p 11. □

Finding Parts

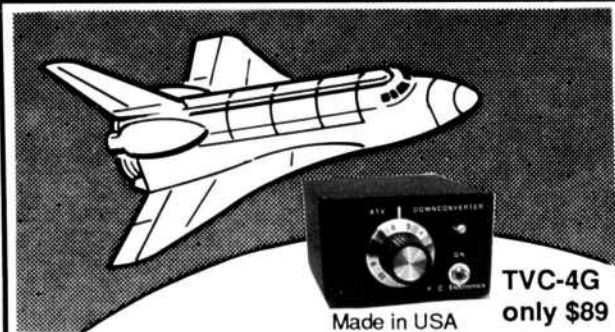
Crystals: The most consistent results were obtained using crystals from Fox Electronics (Tel: 813-693-0099), part number: FOX080. These are series-resonance microprocessor crystals in an HC49/U case. Ask for a list of distributors in your area.

Capacitors: Use monolithic ceramic capacitors from Panasonic or equivalent quality capacitors. Panasonic capacitors are available from Digi-Key Corporation (Tel: 800-344-4539), P4800 series. COG ceramic parts are recommended for good temperature stability. Low loss is an important requirement. 5% or 10% tolerance is acceptable.

Transformer cores: Use two-hole balun cores, part number: BN-43-2402 from Amidon Associates (Tel: 310-763-5770).

Board: The project board, with a ground plane on one side, is part number 8007 from Vector (Tel: 800-423-5659; 800-426-4652 inside California). The Vector pins are part number T44. (Digi-Key is one of the nationwide distributors for Vector.)

AMATEUR TELEVISION



Made in USA

**TVC-4G
only \$89**

SEE THE SPACE SHUTTLE VIDEO

Many ATV repeaters and individuals are retransmitting Space Shuttle Video & Audio from their TVRO's tuned to Spacenet 2 transponder 9 or weather radar during significant storms, as well as home camcorder video. If it's being done in your area on 420 - check page 501 in the 94-95 ARRL Repeater Directory or call us, ATV repeaters are springing up all over - all you need is one of the TVC-4G ATV 420-450 MHz downconverters, add any TV set to ch 2, 3 or 4 and a 70 CM antenna (you can use your 435 Oscar antenna). We also have ATV downconverters, antennas, transmitters and amplifiers for the 400, 900 and 1200 MHz bands. In fact we are your one stop for all your ATV needs and info. We ship most items within 24 hours after you call. **Hams, call for our complete 10 page ATV catalogue.**

(818) 447-4565 m-f 8am-5:30pm pst.

Visa, MC, COD

P.C. ELECTRONICS

Tom (W6ORG)

2522 Paxson Ln Arcadia CA 91007

Maryann (WB6YSS)

High-Performance Antennas for 5760 MHz

You've seen lots of equipment for 5760 MHz described in QEX. Here are some antennas to connect it to.

By Paul Wade, N1BWT

In the recent series "Practical Microwave Antennas," the measurements and most of the examples were for 10 GHz, as that band has become relatively popular since the inception of the 10-GHz Cumulative Contest.^{1,2,3} Some of our other microwave bands have received less attention, particularly 5760 MHz. Recent articles in *QEX* have described some equipment for this band, but there is little specific information available on antennas.^{4,5,6}

While I was working on 10-GHz feedhorns for the "Practical Microwave Antennas" articles, I was also working with the late Don Cook, K1DPP, on feedhorns for 5760 MHz. However, I did not want to publish these designs until I was able to mea-

sure their performance and verify that they actually work. Recently, KB1VC, WB1FKF and I set up an antenna range for 5760 MHz to measure the feedhorns and compare them with some previously published designs.

Measurements

The antenna range used the same superheterodyne ratiometry technique and setup described in "Practical Microwave Antennas, Part 3." Different mixers and filters were required, so we used home-brew mixers with integrated pipe-cap filters.⁷ We were able to make measurements with only one milliwatt of transmitter power by adding a 30-MHz amplifier before the PANFI; the ability to add gain at a low frequency is a real advantage of the superheterodyne technique.

Measurement results are shown in Table 1. We did not have a standard-gain antenna available for 5760 MHz so we used two horn antennas as a gain

reference. The *HDL_ANT* computer program described in the "Practical Microwave Antennas" series uses an algorithm for the gain of a horn that has proved quite accurate at 10 GHz, so we carefully measured the physical dimensions of the two horns in order to calculate their gain. When the gains were measured, we found a discrepancy of 0.6 dB in the gain of one horn relative to the other. Since we do not have a standard, there is no way to determine which is in error, so we split the difference. Therefore, the results shown in Table 1 are either 0.3 dB high or low, depending on which horn gain is incorrect, but this is still a small uncertainty for amateur measurements. An uncertainty of 0.3 dB translates into a range of possible efficiencies of 57% to 66% for the highest gain shown, listed as 61%, and a smaller range for lower efficiencies.

A note on measurement technique: we try to do blind measurements, where one person takes the readings

161 Center Road
Shirley, MA 01464
e-mail: N1BWT@iii.net(Internet)

and another writes them down, with calculations done later, to limit the human tendency to find the "expected" result.

Dish Feeds for 5760 MHz

The whole point of these measurements is to find efficient feeds for a parabolic dish. Table 1 lists the results

and shows several feeds with significantly better performance than previously published designs. Let's discuss them individually:

- WA3RMX triband feed:⁸ Like all multiband antennas, this one is a compromise, and performance is significantly less than an optimum feed—less than 20% efficiency on a

dish with $f/D = 0.45$. The original *QST* article suggests an f/D in the 0.25 to 0.4 range, which would be illuminated more efficiently but probably not with better than 30% efficiency. However, many successful contacts have been made using this feed, and it is highly recommended if a multiband antenna is the only way to get a station on 5760 MHz.

- Cylindrical waveguide feed horn: This was described by W0PW in *QEX* with versions for 3.456, 5.76, and 10.3 GHz.⁹ WB1FKF made a copy of the 5760-MHz version, and we measured it on the recommended dish as well as on two others, all with $f/D = 0.45$. In all cases, the efficiency was 20 to 24%.

Like many folks getting started on a new band, WB1FKF copied the published dimensions but had no test equipment to check it out. Since he was able to make successful contacts with it, he assumed it was working well. After we found that the efficiency was rather low, he checked the return loss and found it to be 5 dB ($VSWR \approx 3.5$). The possible reflection loss for this mismatch is 1.65 dB, so the actual gain could be that much higher if the feed were perfectly matched. The resultant efficiency could then be as high as 35%.

Even though Don copied the published dimensions carefully, it is not surprising that the VSWR was high. This feed uses an E-field probe to excite the circular waveguide, and I have found the impedance of these probes to be extremely sensitive to their dimensions. The Kumar feed, below, also uses a probe to excite the circular waveguide, and it took a fair amount of cut-and-try to find the best combination of length and diameter for the probe.

- Kumar feed:¹⁰ This scalar feedhorn has been described by VE4MA for 1296, 2304 and 3456 MHz.^{11,12} I scaled the dimensions for 5760 MHz as shown in Fig 1, and K1DPP constructed one with compromise dimensions adjusted for available materials—for instance, the outer ring is made from a film can for a 100-foot roll of film. These compromise dimensions are not necessarily optimum. The probe length and diameter are very critical, so copies would probably require some tuning. Performance was excellent, with 61% efficiency on a 25-inch reflector. A later measurement on a

Table 1—Summary of 5.760 GHz Antenna Measurements

N1BWT, KB1VC, WB1FKF 10/29/94			
ANTENNA	FOCAL DIST (inches)	GAIN (dBi)	Efficiency
Horn, Seavy SGA-50 (19.65 dBi calc)		19.3	53%
Surplus AT-802/UPM-9A horn (16.3 dBi calc)		16.6	51%
25-inch dish, $f/D = 0.45$, Satellite City, with the following feeds:			
Clavin feed	11.125	27.5	38%
Clavin feed	10.625	28.3	46%
Clavin feed	10.375	29.2	57%
Clavin feed	10.125	27.9	42%
Kumar (VE4MA) feed (0.25-inch projection)	11.5	29.5	61%
Cylindrical horn feed (1.625-inch ID)		25.3	23%
23-inch dish, antenna center 24 inch, $f/D = 0.45$, with the following feed (24-inch OD but parabolic surface is 23-inch diameter):			
WA3RMX triband feed	10.875	23.3	17%
Cylindrical horn feed (1.625-inch ID)	11	24.5	23%
	10.625	23.7	19%
	11.5	24.7	24%
30-inch dish, $f/D = 0.45$, (lighting reflector), with the following feeds:			
Kumar (VE4MA) feed (0.25-inch projection)	13.9	(29.7)	(42%)
		questionable—see text	
Rectangular horn, (optimum for $f/D = 0.47$) E=1.37 inch, H=1.6 inch			
	13.125	31.1	58%
	12.31	29.1	} focal sensitivity
	13.62	29.1	
Cylindrical horn feed (1.625-inch ID)	13.0	26.5	20%
Waveguide to coax transitions:			
WR-137 round flange (3.12-inch flange OD; FXR C601B)	13.625	30.9	56%
WR-137 rect. Flange (2.25 × 1.5-inch flange)	14.25	30.1	46%
WR-159 rect. Flange (2.5 × 1.75-inch flange; marked 549-033489-001 Rev E; waveguide has rounded inner corners, radius 0.25 inch)	12.625	31.3	61%
WR-187 round flange (3.62-inch flange OD; Waveline 301-NF)	12.5	31.1	58%

Range length = 110 feet. $2D^2/\lambda = 73$ feet. Test height ≈ 10 feet.

Focal distance: each feed was adjusted for maximum gain, except the WA3RMX triband feed, which was not adjustable and was measured to specified phase center. All other focal distances measured to outermost point.

30-inch reflector of the same f/D was much worse—apparently something went wrong.

- Clavin feed:¹³ I scaled the dimensions for 5760 MHz as shown in Fig 2 from my 10368-MHz version (see note 2), and K1DPP machined one. The critical dimension is the slot length, which I filed for best VSWR. This feed also showed very good performance with 57% efficiency. Unfortunately, the dimensions do not fit any readily available materials.
- Rectangular feed horn:¹⁴ My initial estimate of the f/D for the 30-inch reflector was 0.47, so I designed a rectangular horn for an $f/D = 0.47$. The *HDL_ANT* program generated the horn template shown in Fig 3,

which I used to make a horn of flashing copper. The horn, soldered to a piece of WR-137 waveguide, provides very good performance with 58% efficiency. The calculated phase center is 0.02 wavelengths inside the mouth of the horn so we can get a better estimate of the focal point than that found by fitting paper templates generated by *HDL_ANT*.

- Waveguide-to-coax transitions: At 10 GHz, we found that a WR-90-to-coax transition provides about 42% efficiency when used as a dish feed. This is valuable data because it is something readily available for comparisons if there are no antennas with known gain available. For 5760 MHz, there are three usable

sizes of waveguide, and I found coax transitions for all three in my collection acquired at hamfests. We were surprised to find how well these worked: a WR-137 transition with a small rectangular flange provided 46% efficiency, close to our expectation, but transitions with large circular flanges showed much higher efficiencies: 56 and 58%. Finally, the highest efficiency was a WR-159 transition with rounded, rather than square, corners on the inside of the waveguide. While large circular flanges may provide the same effect as the choke flange for cylindrical waveguide feed horns described by WA9HUV,¹⁵ we can offer no explanation for the performance of the rounded corner waveguide transition.

Recommendations

All the dishes we had available have an f/D ratio of 0.45. At this f/D , the Kumar, Clavin and rectangular feedhorn all offer very good performance. For dishes with other f/D ratios, the recommendations are the same as those offered in "Practical Microwave Antennas, Part 2"; the Kumar and Clavin feeds are better for the f/D range of 0.35 to 0.45, while rectangular feedhorns may be optimized for any f/D greater than 0.45. If you find a surplus waveguide-to-coax transition, it may provide performance as good as the ones we measured, but be sure to adjust it carefully; as Table 1 shows, the focal distances, and thus the apparent phase centers, vary widely.

At 5760 MHz, the focal length of the dish is not quite as critical as at 10 GHz since a wavelength is nearly twice as long. However, two of the feeds in Table 1 were measured with varying focal distance to show the loss associated with small focal-length errors. Getting the feed exactly at the focal point is still the most important aspect of dish efficiency and gain.

Finally, match the impedance of the antenna to the transmission line—a low VSWR is important at all frequencies, and even more so at microwaves where transmission line losses are high. In "Practical Microwave Antennas" I made the assumption that this would be obvious, but our measurements here are a reminder that the obvious sometimes needs restatement.

Conclusion

It should be apparent that signifi-

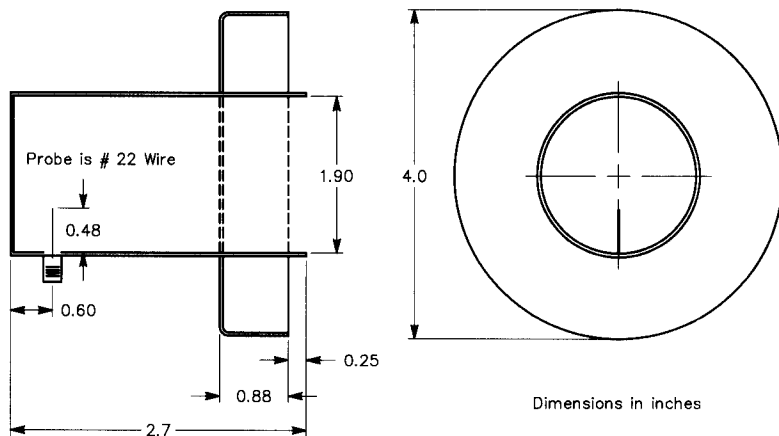


Fig 1—Kumar feed for 5760 MHz. Dimensions may not be optimum. An SMA connector is used.

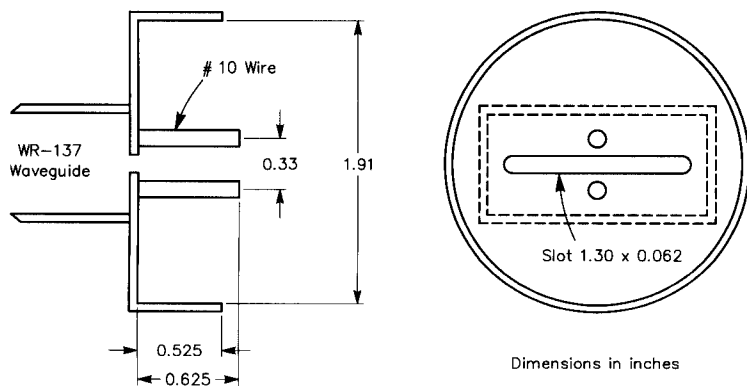


Fig 2—Clavin feed for 5760 MHz.

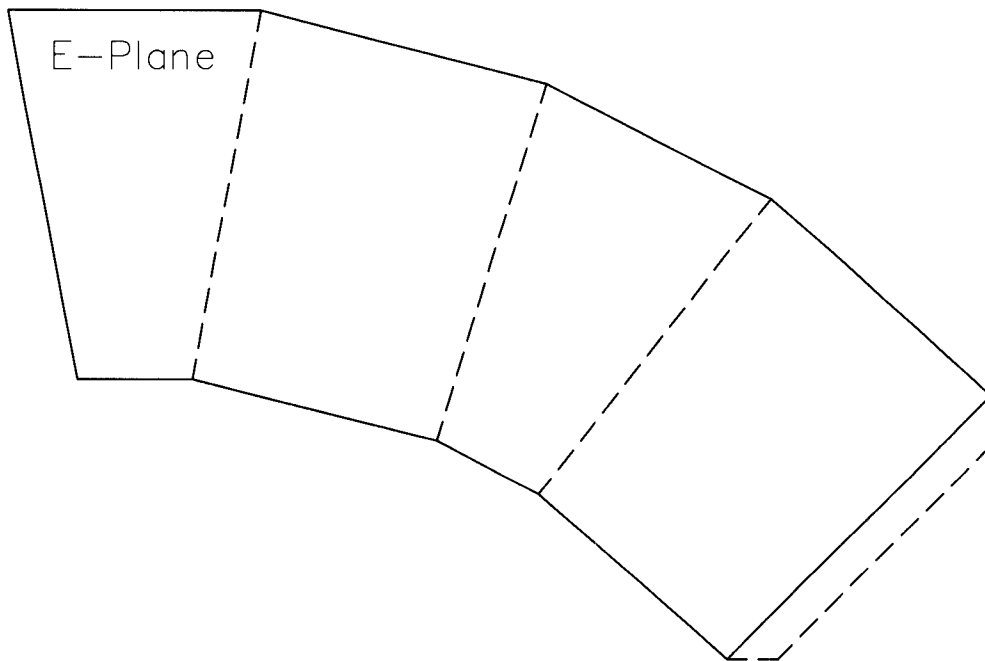


Fig 3—Full-size template for a 7.2-dBi horn for 5760 MHz, suitable for illuminating a dish with $f/D=0.47$.

cant improvements in dish efficiency are available, compared to previously published feed designs for 5760 MHz. How significant? The measurements show a gain increase of 3 to 4 dB with no increase in dish size, weight or wind loading—enough to double the range of a pair of stations making this improvement.

Acknowledgment

Don Cook, K1DPP, provided both enthusiasm and machining skills for this project. Unfortunately, he became a Silent Key before it was completed. He was a true friend and helped all the hams who knew him; we all miss him.

Notes

¹Wade, P., N1BWT, "Practical Microwave

Antennas, Part 1," *QEX*, September 1994, pp 3-11.

²Wade, P., N1BWT, "Practical Microwave Antennas, Part 2," *QEX*, October 1994, pp 13-22.

³Wade, P., N1BWT, "Practical Microwave Antennas, Part 3," *QEX*, November 1994, pp 16-24.

⁴Lau, Z., KH6CP/1, "A 5616-MHz Local Oscillator," *QEX*, May 1993, pp 15-19.

⁵Cook, R., N2SB, "5760 MHz from the Junkbox," *QEX*, May 1994, pp 20-24.

⁶Lau, Z., KH6CP/1, "A Low-Noise PHEMPT Amplifier for 5760 MHz," *QEX*, September 1994, pp 28-31.

⁷Wade, P., N1BWT, "Mixers, Etc., for 5760 MHz," *Proceedings of Microwave Update '92*, ARRL, 1992, pp 71-79.

⁸Hill, T., WA3RMX, "A Triband Microwave Dish Feed," *QST*, August 1990, pp 23-27.

⁹Hilliard, D.L., W0PW, "Antenna Ideas for 3.5, 5.8, and 10.3 GHz," *QEX*, January 1988, pp 3-5.

¹⁰Kumar, A., "Reduce Cross-Polarization in Reflector-Type Antennas," *Microwaves*, March 1978, pp 48-51.

¹¹Malowanchuk, B. W., VE4MA, "Selection of an Optimum Dish Feed," *Proceedings of the 23rd Conference of the Central States VHF Society*, ARRL, 1989, pp 35-43.

¹²Malowanchuk, B. W., VE4MA, "VE4MA 3456-MHz circular polarization feed horn," *Feedpoint*, November/December 1991, North Texas Microwave Society.

¹³Clavin, A., "A Multimode Antenna Having Equal E- and H-Planes," *IEEE Transactions on Antennas and Propagation*, AP-23, September 1975, pp 735-737.

¹⁴Evans, D., G3RPE, "Pyramidal horn feeds for paraboloidal dishes," *Radio Communication*, March 1975.

¹⁵Foot, N. J., WA9HUV, "Second-Generation Cylindrical Feedhorns," *Ham Radio*, May 1982, pp 31-35.

□□

Effects of the Ionosphere

Received HF fax images clearly show the distortion imposed on a signal by the ionosphere.

By Jacques d'Avignon, VE3VIA

Seldom do we have a chance to clearly see the effects of the ionosphere on the quality of the received signal. As amateurs, we transmit or receive on one frequency and, if the signal does not "punch through," we change to a different band and try again.

For many years now, I have been involved in the reception of weather maps transmitted by various stations around the world. As the agencies operating these stations do not normally know where the receiving stations will be located, a set of frequencies is used that covers a good slice of the HF part of the spectrum.

At this time (late 1994) the following stations can be easily received in northeastern North America: NAM, CFH, NMF and AFS. All these stations

normally transmit on a minimum of two frequencies at any time.

During the summer of 1993, I noticed some delay in the reception of the various elements of a chart. Distortion was also present in the final product from the above stations. It normally is not possible to receive more than two frequencies at any one time, thus making it very difficult to do a good comparison of the received quality of the signals.

On July 8, 1993, at 0300 UTC, it was finally possible to receive CFH on three discrete frequencies simultaneously. As the frequencies were already loaded in the memory of my receiver, it was a simple matter to swing the dial to tune to a new frequency and keep on receiving the signal. The receiver, a Kenwood R-5000, was located at 44.22N, 76.58W. The antenna used was a horizontal bundle of seven quarter wavelengths cut for various frequencies in the HF spec-

trum, all connected in parallel. The distance between the transmitter and the receiver was just over 1000 km.

The received map, Fig 1, and its enlarged section, Fig 2, clearly display the effects of propagation on facsimile reception and, by extension, on any received signal. The map was received on three discrete frequencies from CFH/Halifax. Each frequency was affected differently by the ionospheric refraction at the time.

Segments A, D and G of Fig 1 were received at 10.536 MHz. The signal registered about S8 on the meter. The vertical lines are sharp, and very little, if any, fading or multipath distortion is apparent in the output.

Segments B, E and H were copied at 6.496 MHz. This signal was the strongest of the three, at about 30 dB above S9. The strength and near-commercial quality of the signal were consistent with the fact that 6 MHz was the calculated optimum working fre-

quency (OWF) for this circuit at the time.

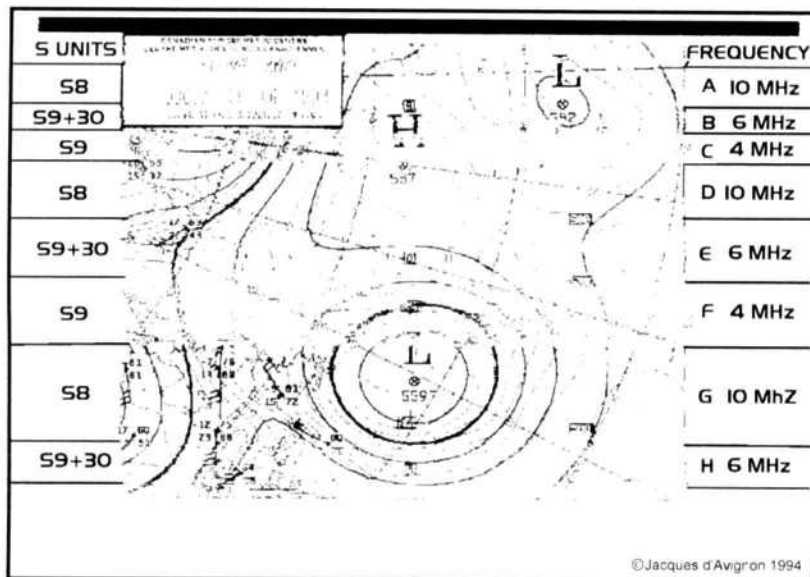
If you closely examine the vertical lines in the 6-MHz segments of Fig 1, you will notice a certain amount of degradation; the vertical lines are not sharp, and in a few spots you will see that segments of these same lines are offset. This offset is caused by the rapid variation of the ionosphere height and/or two or more different signals along different paths being received, causing a time difference in the arrivals of the signals. But it is an acceptable signal, close to commercial quality for weather maps. If this were a transmission of a photograph, it would be of marginal quality.

Now let's look at segments C and F of this chart. These segments were copied at 4.271 MHz. The data is useless! Examine the enlargement of a section of this chart shown in Fig 2 to judge the quality of the received signals at each frequency.

Each pixel in the 4-MHz segments is echoed and cannot be read properly. If you look at the vertical line at the extreme right side in segment F, it is obvious that more than one signal was being received, and the delay between each signal caused the muddy appearance on the chart. But the strength of the combined signals on 4 MHz was very high—close to S9—making it an attractive signal—until you look at the results. In the 4-MHz segments, the signal was being refracted by the ionosphere along multiple paths of different lengths: a one-hop (1F) path off the F layer and a two-hop (2F) path.

This example is most interesting as the best signal was received on a frequency very close to the highest possible frequency (HPF) on a 1F mode for this circuit. (See the attached propagation "hindcasting" data in Fig 3 and Table 2, which was calculated for this circuit.) The worst reception was at a frequency below the calculated OWF. At this frequency (4 MHz) a "mixed modes" propagation condition was calculated by the ASAPS (Advanced Stand Alone Prediction System) program. That means it's likely I was receiving the same signal via more than one mode: a 1F or a 2F mode.

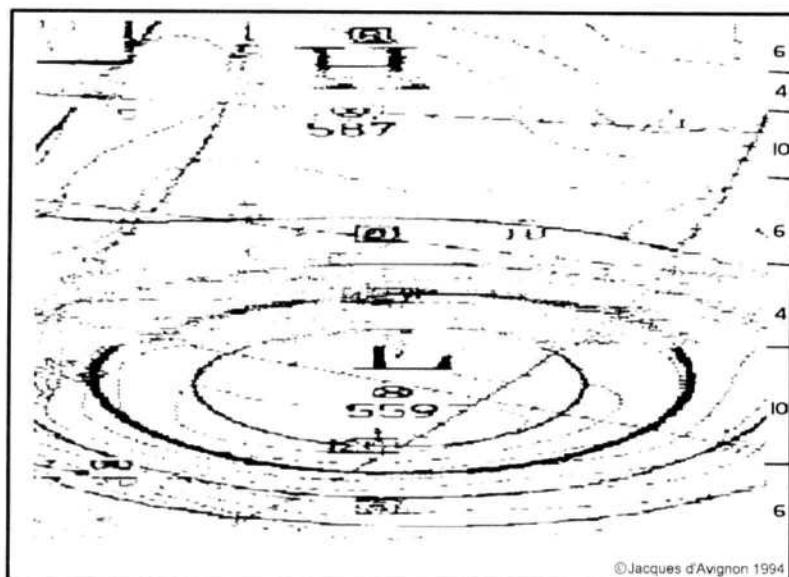
This is obviously what happened on 4 MHz, causing echoing of each pixel. The echoing is a time delay of approximately 2 to 4 milliseconds in the reception of each copy of the pixel. Each pixel was arriving by two transmission paths of varying length. The difference in path length between the 1F and the



EFFECTS OF THE IONOSPHERE ON FAX RECEPTION

INTERCEPT FROM CFH HALIFAX JULY 8, 1993 03:00 UTC

Fig 1



ENLARGEMENT OF A SECTION OF THE CFH MAP. JULY 8, 1993.

Fig 2

2F modes was calculated to be about 800 to 1000 km.

It is interesting to look at the *GRAFEX* predictions of Table 2 for this circuit for the time slot 0300 to 0500 UTC. This is the tabular output of the graph presented in Fig 3. The 6-MHz frequency was near the OWF in the first mode, but *ASAPS* was predicting a possible mixed mode (M) comprising both 1F and 2F propagation at this time. This would explain a certain amount of echoing visible on the received image in the 6-MHz segments.

To avoid this echoing on 6 MHz, it would have been necessary to have an antenna with a vertical main lobe that could sharply discriminate between the 1F arrival angle of 23 to 36 degrees and the 2F arrival angle of 43 to 57 degrees.

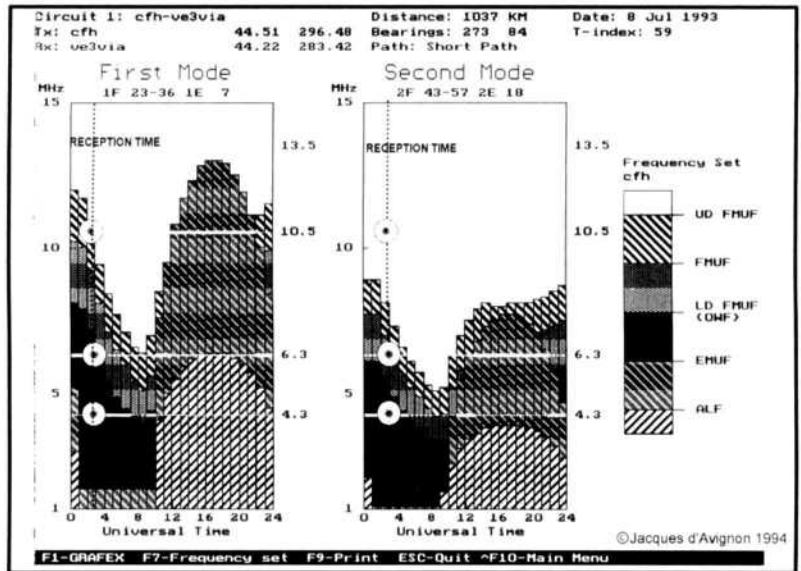
In this example, the best quality signal was at 10 MHz. This frequency was very close to, but still below, the calculated HPF for the 1F mode, but was well above the HPF for the 2F mode. (See Table 2.)

I have been trying to obtain some ionosounds for this path—or a path very close to it—in order to make a good study of this case. But it appears that the only possible sounding station does not have any data available for that date, so many of my conclusions are made from the data available and, in some cases, by deduction.

In March of 1994, I submitted a copy of the original analysis of this case to George H. Hagn of SRI International for his comments. He responded, in part: "I believe that it is more likely that two (or more) signals along different paths are the cause rather than a rapid variation of ionospheric height. In addition to one-hop and two-hop F modes, the upper (Pedersen) ray may have been strong enough to give differential delay."

On the subject of the hindcasting data, Mr. Hagn notes that it is difficult to say if 10 MHz is just above or just below the basic MUF (BM). I have to agree that my conclusion that it is just below the MUF could be proven inaccurate, but without proper sounding data it is difficult to make a clear determination of where the MUF is located.

Mr. Hagn did make another very interesting observation: "The multiple-hop modes may not have arrived



"HINDCASTING" OF THE IONOSPHERIC CONDITIONS ON JULY 8, 1993

Fig 3

Table 1—HF Fax Stations and Frequencies

Station	Location	Frequencies (MHz)
NAM	Cutler, ME	3.357, 8.080, 10.865, 15.959, 20.015
NMF/NIK	Cape Code, MA	6.340, 12.750
CFH	Halifax, NS	0.1225, 4.271, 6.496, 10.536, 13.510
AFS	Elk Horn, NE	3.232, 4.858, 5.908, 6.905, 11.122, 19.327

on a great-circle path. Have you considered the effects of non-great-circle propagation? As you know, the 1F2 mode (low ray) is most likely to be along the great-circle path; whereas, if there are ionospheric gradients, the paths of the higher-order modes will be deviated from the great-circle bearing as mode order increases."

The study of this case has been most interesting and has certainly raised many questions. There are still many areas in the field of ionospheric propagation that need research. I believe that any amateur operator or short-wave listener can document any unusual propagation case and try to do an interpretation of what happened.

RF

By Zack Lau, KH6CP/1

A 1296-MHz Cavity Preamp

One of the neat things about attending VHF and microwave conferences is the exchanges of ideas that happen there. A good example occurred at the 1992 Central States VHF conference held in Kerrville, TX. I showed off a 2-meter preamp that uses half-inch Andrew Helix for the resonator. To my surprise, it beat all of the cavity preamps. Perhaps impressed by my efforts, Jim Vogler, WA7CJO, suggested I try building a preamp with a half-wave cavity to get a lower noise figure (NF). I did so, demonstrating 903 and 1296-MHz preamps at the 1992 Microwave Update in Rochester, NY. Jim has supplied drawings of a (somewhat modified) version of the half-wave cavity I used (Fig 1), along with his own preamp circuit for 903 and 1296 MHz (Fig 2). My 1296-MHz circuit is shown in Fig 3.

I built two 1296-MHz GaAs FET preamps that give measured noise figures of around 0.34 to 0.43 dB, depending on whose meter you use, with a gain of around 15 dB. Their noise figures measure only a few hundredths of a dB worse than the best PHEMT designs, indicating the superiority of the approach; the improved input circuitry almost makes up for the

noisier GaAs FET used in this design.

The advantage of the half-wave cavity over microstrip or coax resonators is its higher unloaded Q, which allows the required impedance transformation to be obtained with less loss. This translates into lower noise figure because the noise figure of a preamplifier is basically the noise of the transistor plus the noise added by the input network—other noise contribu-

tions are usually minimal, at least when dealing with high-gain devices.

A common misconception is that the cavity has to be silver plated to work well; bare copper works just fine. What does help is polishing the inside metal surface with steel wool to get an exceptionally smooth surface. Rough surfaces degrade the Q and increase the loss. I used silver-plated brass tubing for the center conductor because it

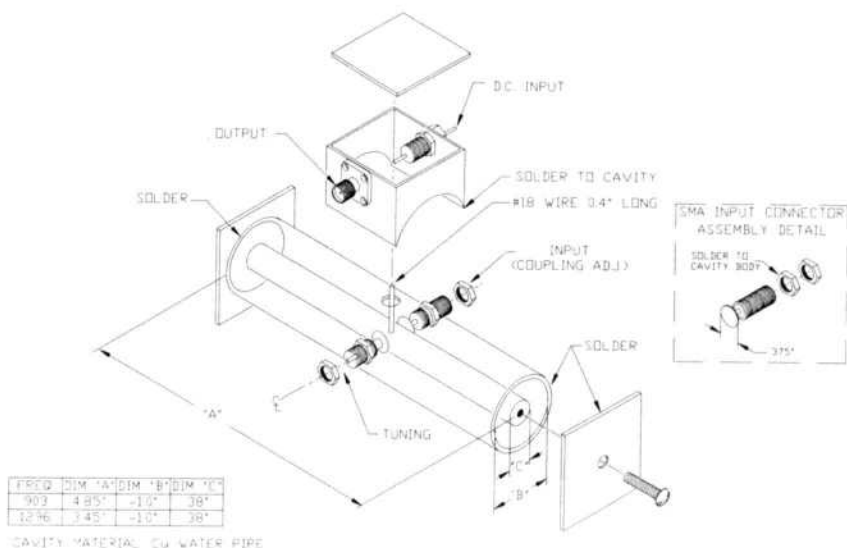


Fig 1—WA7CJO's drawing of the half-wave coaxial cavity low-noise preamplifier.

225 Main Street
Newington, CT 06111
e-mail: zlau@arrl.org (Internet)

wasn't much work to silver plate it with Cool-Amp silver-plating powder.¹ Had I not had an expensive bottle of this powder around, I'd probably have used copper tubing instead. The brass tubing stock I had available is thinner than the copper stock, making soldering easier.

A disadvantage of half-wave cavities is the mechanical complexity of the tuning mechanisms. You need two variable capacitors inside the center of a long tube—the cavity. Designing an effective solution to this need can be like putting a difficult puzzle together. Jim Vogler's approach is shown in Fig 1. Mine is only slightly different.

I first prepared the cavity by drilling and tapping the holes for the input connector and the tuning capacitor screw. The hole for the tuning capacitor is tapped with a 10-32 thread, while the hole for the SMA input connector is tapped with a ¼-36 thread. Since copper doesn't hold threads very well, I soldered nuts to the copper. I used a stainless steel SMA connector to hold the ¼-36 nut during the soldering operation. Stainless steel doesn't take solder easily, so it was easy to remove the connector after soldering. The interior end of the

SMA connector is attached to a copper disk that acts as one plate of the input coupling capacitor. I soldered the capacitor plate to the SMA connector and then threaded it into place. A big unknown in a preamp design such as this is the required range of capacitance. PHEMTs typically need a higher impedance transformation, which means less capacitance than for GaAs FETs. A long SMA barrel might work better than the connector I used, as it will give more capacitance adjustment range. In Jim's version, a similar plate is soldered to the end of the tuning screw mounted on the side of the cavity opposite the input connector. For my cavity, I simply use a nickel-plated brass screw with the head sanded flat—no additional disk is needed.

Assuming you have managed to get the tweakers in place, it is pretty easy to solder the output wire to the center conductor tubing and then to solder this assembly in place with some copper end plates. If you guessed wrong on the input capacitance range, you can move the end plates a little to compensate during initial tune-up. The center conductor will then be slightly off-center, which is okay.

One obvious question is: Why not use a PHEMT device for better per-

formance? It is certainly worth trying, but the challenge with PHEMTs is obtaining stability at low microwave frequencies. I've actually seen a PHEMT preamplifier with a positive input return loss. Yes, it actually returned more power than was fed into it. Despite its astoundingly low noise figure, I didn't consider it to be a useful design for EME work. Ideally, I like to see preamps tested for broad-band stability with vector network analyzers, but these are even tougher to find than NF meters!

The input impedance transformation for best NF with PHEMTs is often quite a bit higher than for GaAs FETs. This usually results in higher gain, making the preamplifier more difficult to stabilize. A more direct disadvantage is the added input-network loss that results as you increase the transformation. Unlike FET manufacturers, you are concerned about the achievable noise figure, as opposed to the device noise figure. A 0.05-dB NF device is of little use if any real matching network incurs 2 dB of loss! You may as well use a GaAs MMIC to make a 2-dB NF, 1296-MHz preamp.

Finally, you have to watch the $1/f$ noise of the device you are using. $1/f$ noise, from a practical engineer's point of view, limits how low in fre-

¹Notes appear on page 29.

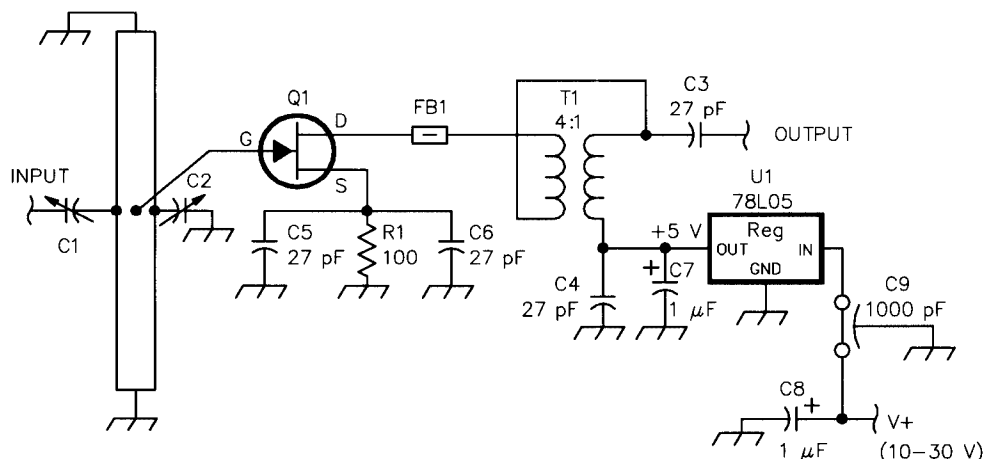


Fig 2—Schematic diagram of the WA7CJO preamplifier.

C1—A 0.7-inch diameter, 20-mil thick copper disk attached to the SMA connector.
C2—A 0.7-inch diameter, 20-mil thick copper disk attached to a 10-32 brass flat-head screw.

C3-C6—0.05 × 0.05-inch chip capacitors.
FB1—Ferrite bead. Optional, may reduce the tendency of the circuit to oscillate.
Q1—MGF1402, MGF1412, ATF10135 or similar GaAs FET.

R1—100-Ω nominal, adjust to get 8 to 15 mA of drain current.
T1—4:1 balun. 3 turns #32 enam wire, bifilar wound on a Siemens B62152-A0008-X060 double-aperture core.
U1—78L05 5-volt regulator IC.

quency you can use the device. If you look at NF versus frequency you see a bathtub shaped curve. The difference between an ordinary PHEMT and a GaAs FET is that the NF curve has been moved upward in frequency. Unfortunately for 432 EME aficionados, as devices get improved for better 12-GHz performance their operation at 432 MHz is likely to suffer. One well-known EMEer has commented that the early batches of a certain PHEMT were great, but more recent batches have been disappointing. So, you have to be careful, as those NF curves actually go back up as you go lower in frequency, even though some manufacturers make it look as though the NF approaches zero at low frequencies. This is why you see silicon MOSFETs used at HF and JFETs used at audio: the $1/f$ noise curves dictate these selections.

The device I chose for this preamp is the Hewlett Packard ATF 10135 GaAs FET. I've had good luck making stable 1296-MHz preamps with this device, a

definite bonus when trying out design concepts. I had no difficulty in using source biasing. I think source biasing has several advantages, the most important being the ability to optimize the gate circuit with respect to input losses. Introducing a negative bias voltage on the gate often involves potentially lossy decoupling circuitry. Simplicity is another benefit, especially if you intend to build several preamps and choose the best one. Of course, source biasing requires proper design of the source bypasses.

Proper RF bypassing of the source leads is a tricky subject to tackle. It is best done by a computer-aided stability analysis, although acceptable designs can be obtained via trial and error. I've had good luck in source biasing preamps all the way up to 3456 MHz using 50-mil chip capacitors. It may be possible to go even higher in frequency if smaller capacitors are used. The advantage of physically smaller capacitors is lower stray inductance, which gives you more flex-

ibility in how much you can vary the total inductance with your lead length. Adding up the inductances present is a convenient way to look at the situation, but if your initial design doesn't work you should consider looking more deeply into the situation, perhaps using transmission line—or even more sophisticated—models. One of the keys to intelligent design is effectively trading-off model accuracy with an understanding of what is going on. True, you can sometimes get lucky and design something that works really well if you don't understand the details, but I find that the more you know, the easier things are to optimize.

Fortunately for those of us looking for variables to tweak for stability, you can also play with the drain or output circuit. Here we have lots of flexibility since we can often toss gain away. Designers sometimes use fancy networks to precisely control the impedance over wide frequency extremes. Instead, I just used a 47- Ω resistor

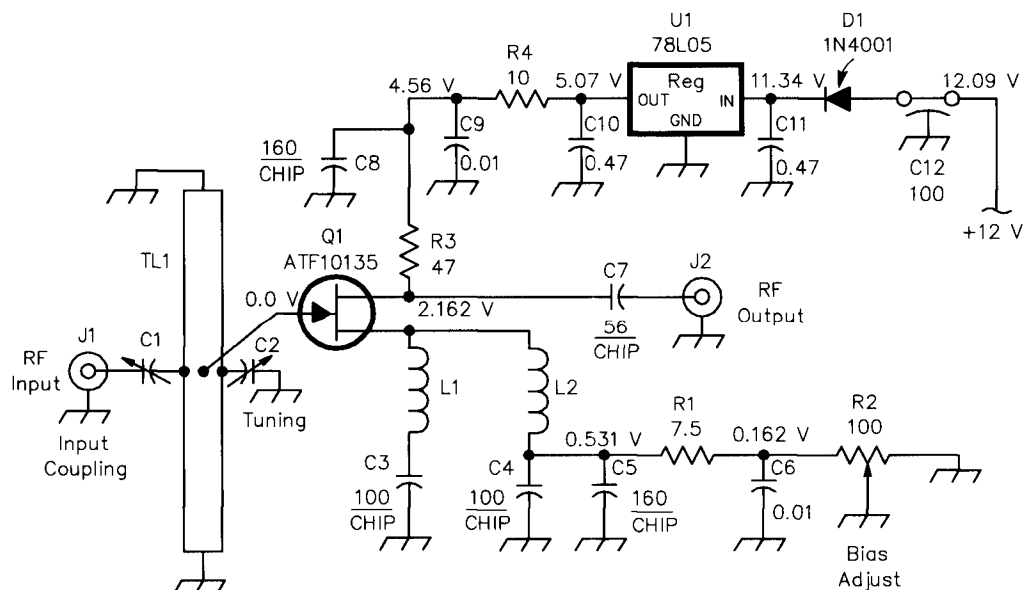


Fig 3—Schematic diagram of the KH6CP 1296-MHz preamplifier.

C1—A 0.7-inch diameter, 20-mil thick copper disk attached to the SMA connector.
 C2—The sanded-flat head of the 10-32 tuning screw forms one plate.
 C3, C4—100-pF, ATC 100A chip capacitors. See text regarding substitution.
 C5—160-pF, ATC 100B chip capacitor. This capacitor may not be needed.

C7—56-pF, ATC 100B. A relatively noncritical coupling capacitor.
 C8—160-pF, ATC 100B chip capacitors.
 L1, L2—80-mil lead length of the FET to the center of each capacitor.
 Q1—ATF10135 low-noise GaAs FET.
 R1— $\frac{1}{4}$ -W carbon composition resistor, available from Mouser Electronics (see Note 2).

TL1—Coaxial resonator. The outer conductor is a 3.38-inch length of 1.05-inch (inside diameter) copper water pipe. The inner conductor has a diameter of 0.375 inches.
 U1—78L05 5-volt regulator IC.

strapped across the output, which was good enough to get a working preamplifier. A fancy network might help improve stability if you find you need it. What you *don't* want is an adjustable network—unless you have a straightforward means of adjusting it. A preamplifier with four interactive tuning controls is great for people who want to spend all winter tweaking preamps—and downright annoying for those waiting in line to use the NF meter at a conference! (The Eastern States conference has been fortunate in having two meters available so one can be used for tweaking while the other is used for official measurements.)

Tuning a cavity preamplifier can be time consuming, even with an NF meter. Normally, you want to adjust the input coupling first, then adjust the tuning for best performance. As you increase the input coupling, the gain should rise while the noise figure drops. The noise figure will often reach a minimum after the gain peak. Finally, with too much input coupling, the gain will drop and the noise figure will rise. You normally tune for minimum noise figure, though you might want to undercouple the input for better selectivity. After you're done, it might be a good idea to measure the input return loss if you can do so. You shouldn't expect too good of a match—perhaps a couple of dB of return loss and perhaps as much as -5 or -6 dB at lower frequencies. But a *positive* return loss indicates the need for more work. I saw this happen with a 903-MHz preamplifier so I rebuilt it using the 50-mil chip capacitors I suggested previously, even though they are tougher to get than the 110-mil chip capacitors I used originally. This eliminated the problem.

The tuning process I just described can result in a highly unfortunate error. If you attempt to tune up the preamplifier without tightening up the lock nuts, you may discover that the preamp doesn't do better than about 0.7-dB NF. Yes, the extra losses caused by loose contacts can actually be that high. The problem is primarily in the tuning capacitor, rather than the input coupling capacitor. Of course, if the lock nuts are tight you can't easily tune the preamplifier. As I said, this can be a time-consuming process.

The source bias shown in Fig 3 is best preset to the manufacturer's recommended bias current level. For the

ATF 10135, this is 25 mA. You can measure the voltage across R1 to determine the bias current. However, I bought a batch of transistors and found they all worked best with a current of 40 to 50 mA. This is quite a bit higher than I expected.

Stabilizing NF Measurements

Al Ward, WB5LUA, has a neat idea for those marathon noise figure sessions—he put his Hewlett Packard 346A noise source in a vise. This acted as a heat sink, preventing the noise source from warming up too much and increasing the NF meter reading. The HP 8970 noise figure meter also has a command to reset the reference temperature—if you are willing to wait for the source to warm up. The error is perhaps 0.05 dB under typical conditions.

Paralleling Coax

In the November/December 1983 issue of *RF Design*, Bob Zavrel, W7SX, implemented a transmission line transformer using two paralleled 12.7-inch lengths of RG-58A/U coax to get a nominal 12.5 to 50- Ω transformation.³ A 50-pF tuning capacitor on the paralleled center conductors provides a bit of tuning adjustment to compensate for the capacitive reactance of the exotic DVD150T FETs he used, while

a 0.1- μ F coupling capacitor connects the paralleled shields to ground. By coiling the coax, Bob made this 146-MHz transformer also function as a balun.

Obviously, the velocity factor of the coax shortens the length of coax required. Not quite as obvious is the effect of paralleling coax on loss. According to research I've done, the loss of a paralleled cable is the same as that of a single run of coax of the same length, assuming that both cables are properly matched to the source and load. That is, the loss through paralleled 1-foot lengths of coax is the same as the loss through a single 1-foot cable of the same kind. (However, mismatches in electrical length tend to increase the loss.) Thus, a parallel transmission line made from two lengths of coax, while good from a shielding point of view, doesn't exhibit the extremely low losses expected of good open-wire transmission line.

Notes

¹Cool-Amp Conducto-Lube Company, 15834 Upper Boones Ferry Road, Lake Oswego, OR 97035-9948. Tel: 503-624-6426.

²Mouser Electronics, 2401 Hwy 287 N, Mansfield, TX 76063. Tel: 800-346-6873.

³Zavrel, B., "A High-Power VHF FET Amplifier," *RF Design*, Nov/Dec 1983, pp 32-34.

□□



QEX Subscription Order Card

**American Radio Relay League
Newington, CT USA 06111-1494**

For 12 issues of QEX in the
US

- ARRL Member \$12.00
 Non-Member \$24.00

In Canada, Mexico and US by
First Class Mail

- ARRL Member \$25.00
 Non-Member \$37.00

Elsewhere by Airmail

- ARRL Member \$48.00
 NonMember \$60.00

Elsewhere by Surface Mail
(4-8 week delivery)

- ARRL Member \$20.00
 NonMember \$32.00

Remittance must be in US
funds and checks must be
drawn on a bank in the US.
Prices subject to change
without notice.

QEX, The ARRL Experimenter's Exchange is available at the rates shown at left. Maximum term is 12 issues, and because of the uncertainty of postal rates, prices are subject to change without notice.

Renewal New Subscription

ARRL Membership Control # _____

Name _____ Call _____

Address _____

City _____ State or
Province _____ Postal
Code _____

Payment Enclosed

Charge
 MasterCard VISA American Express Discover

Account # _____ Good thru _____

Signature _____

Date _____